

A Certified Goal-Oriented A Posteriori Defeaturing Error Estimator for Elliptic PDEs

Philipp Weder^{1,†} and Annalisa Buffa^{1,*}

¹ *Institute of Mathematics, Ecole Polytechnique Fédérale de Lausanne,
Station 15, CH-1015, Lausanne, Vaud, Switzerland*

[†]philipp.weder@epfl.ch, ^{*}annalisa.buffa@epfl.ch

December 24, 2025

Abstract

Defeaturing, the process of simplifying computational geometries, is a critical step in industrial simulation pipelines for reducing computational cost. Rigorous a posteriori estimators exist for the global energy-norm error introduced by geometry simplifications. However, practitioners are usually more concerned with the accuracy of specific quantities of interest (QoIs) in the solution. This paper bridges that gap by developing mathematically certified, goal-oriented *a posteriori* defeaturing error estimators for Poisson's equation, linear elasticity, and Stokes flow. First, we derive new reliable energy-norm estimators for features subject to Dirichlet boundary conditions in linear elasticity and Stokes flow, based on existing results for Poisson's equation. Second, we formulate general energy-norm estimators for multiple negative features, subject to either Dirichlet or Neumann boundary conditions for the first time. Finally, we combine these estimators with the dual-weighted residual (DWR) method to obtain reliable estimates for linear QoIs and demonstrate their effectiveness across a range of numerical experiments.

Keywords: Geometric defeaturing; goal-oriented error estimation; a posteriori error analysis; dual-weighted residual method.

AMS Subject Classification: 65N50, 65N15, 65N30

1. Introduction

Solving partial differential equations (PDEs) in industrial applications often involves geometrically complex domains. These geometries contain features across multiple scales, which makes meshing difficult and simulations computationally expensive. Even the presence of a single, relatively small geometric feature can increase the computational cost of a simulation by an order of magnitude due to the need for additional degrees of freedom.^{23,39} It is standard practice to simplify these geometries by removing small or irrelevant features, a process known as defeaturing.

Traditionally, defeathering relies on *a priori* criteria that are applied before any simulation is performed. These criteria are often heuristic, ranging from an engineer’s subjective expertise²² to simplifications based on purely geometrical rationale³⁴ or prior knowledge of the underlying physical problem.^{13, 14, 31}

For a certified modeling and simulation process, *a posteriori* defeathering error estimators are necessary. Early approaches provided the crucial insight that the error concentrates at simplified boundaries¹² or were based on asymptotic considerations such as feature sensitivity analysis (FSA), which crucially rely on the assumption of infinitesimally small features.^{17, 18, 35, 36} More recent methods using the dual-weighted residual (DWR) technique^{4, 30} or the reciprocal theorem have also been explored.^{25, 26, 33, 40} However, these works lack a rigorous mathematical certification and involve heuristic parameters that depend on the feature’s size.

This work builds on the framework for *a posteriori* defeathering error estimation introduced by Buffa et al.,⁷ where the defeathering problem is rigorously analyzed for the Poisson problem with one feature subject to Neumann boundary conditions. It provides estimates that explicitly capture the size of the feature, allowing for the treatment of features of any size. Subsequent work extended this framework in several directions: Antolín and Chanon² generalized the estimates to multiple features with Neumann boundary conditions, as well as to the linear elasticity and Stokes’ equations. Weder and Buffa³⁸ treated the case of negative features subject to Dirichlet boundary conditions for Poisson’s equation. Furthermore, Buffa et al.^{6, 8, 9} combined the defeathering estimators with *a posteriori* numerical error estimators for isogeometric analysis^{21, 28} and finite elements. Chanon¹⁰ provides a comprehensive treatment of the topic.

While the previously introduced estimators provide robust estimates of the defeathering error in the global energy-norm of the underlying PDE problem,^{2, 7, 10} engineers are often interested in the accuracy of specific quantities of interest (QoIs), such as the average stress on a surface, the flux across a boundary, or the displacement at a specific point. In the latter cases, the global energy norm may not be an accurate proxy for the error in these QoIs. To bridge this gap, we combine the rigorous energy-norm estimators with DWR.^{4, 30}

This paper makes three primary contributions: First, we extend the analysis of Dirichlet features to linear elasticity and Stokes flow by deriving new reliable energy-norm estimators, which are of independent interest. Second, we present a unified problem formulation for geometries with mixed Dirichlet and Neumann features. Building on this foundation, we then develop certified goal-oriented defeathering estimators for linear quantities of interest applicable to all three model problems. Our approach advances beyond previous DWR-based methods, which rely on heuristic approximations or the dismissal of uncomputable error terms.^{25, 26} In contrast, our framework provides a mathematically certified error bound in the form of an inequality up to a constant that is independent of the feature’s size. Moreover, it is significantly more general, providing estimators for complex configurations involving multiple negative isotropic features, features on the domain boundary, and those subject to either Dirichlet or Neumann conditions, thus overcoming key limitations

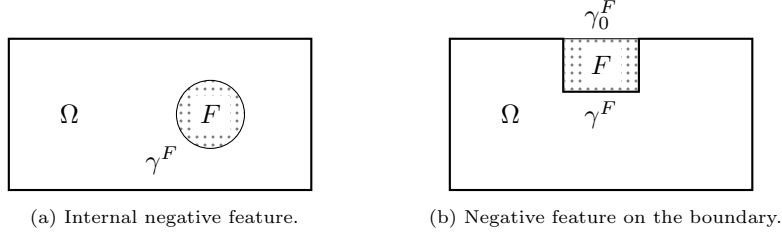


Fig. 1: Domain with an internal feature F (a) and a boundary feature F (b). The defeatured and simplified boundaries are denoted by γ and γ_0 , respectively. The dotted parts represent the feature's interior.

of prior work.²⁶

The paper is structured as follows: Section 2 provides the necessary geometric and functional analytic background. Sections 3 to 5 are dedicated to the Poisson, linear elasticity, and Stokes problems, respectively. For each model, we first formulate the general defeaturering problem for geometries with multiple features and mixed Dirichlet and Neumann boundary conditions, and then derive the corresponding goal-oriented *a posteriori* error estimators. The reliability proofs for the new energy-norm estimators for Dirichlet features in elasticity and Stokes flow are detailed in Appendices B and C, respectively. Finally, we validate our theoretical results with numerical experiments in section 6 and present our conclusions in section 7.

2. Preliminaries

This section provides the necessary background for our analysis, beginning with the terminology used to describe complex geometries with negative features. It then defines the functional spaces in which our analysis is set. We begin by recalling the notation \lesssim : We write $A \lesssim B$ whenever $A \leq cB$ for some constant c independent of the size of the considered domains and boundaries. Additionally, we use $A \simeq B$, whenever $A \lesssim B$ and $B \lesssim A$.

2.1. Domains, boundaries, and features

In what follows, let $\Omega \subset \mathbb{R}^n$ denote a bounded open set. We say that Ω is a Lipschitz domain if its boundary $\partial\Omega$ is locally the graph of a Lipschitz function. Unless otherwise stated, we restrict our analysis to such domains for $n = 2$ or $n = 3$.

Let ω be a d -dimensional submanifold of \mathbb{R}^n with $d \in \{n, n-1\}$. If $d = n$, then $|\omega|$ denotes the Lebesgue measure of the set ω , while for $d = n-1$, $|\omega|$ denotes the $(n-1)$ -dimensional Hausdorff measure. The closure and interior of ω are denoted by $\bar{\omega}$ and $\text{int}(\omega)$, respectively. For a subset $\omega_* \subset \omega$, not necessarily connected, we denote by $\text{hull}(\omega_*)$ the convex hull of ω_* in ω . Moreover, we denote by $\text{diam}(\omega_*)$ the manifold diameter of $\text{hull}(\omega_*)$, that is $\text{diam}(\omega_*) := \max\{\rho(x, y) | x, y \in \text{hull}(\omega_*)\}$, where $\rho(x, y)$ denotes the geodesic distance between two points x and y . Finally, we

will require the geometrical features defined below to satisfy the following isotropy property:

Definition 2.1. *Let ω be a d -dimensional subset of \mathbb{R}^n , $d \in \{n-1, n\}$. We say that ω is isotropic if*

$$\text{diam}(\omega) \lesssim \max_{\omega_c \in \text{conn}(\omega)} (\text{diam}(\omega_c)),$$

and each connected component $\omega_c \in \text{conn}(\omega)$ satisfies $\text{diam}(\omega_c)^d \lesssim |\omega_c|$. In particular, if ω is isotropic and if we let $\omega_{\max} := \text{argmax}_{\omega_c \in \text{conn}(\omega)} (\text{diam}(\omega_c))$, then

$$\text{diam}(\omega)^d \lesssim \text{diam}(\omega_{\max})^d \lesssim |\omega_{\max}| \leq |\omega|.$$

Moreover, if ω is connected, we have $\text{diam}(\omega)^d \simeq |\omega|$.

Next, we will formalize the idea of a feature. Let $\Omega \subset \mathbb{R}^n$ be a Lipschitz domain. As illustrated in Fig. 1, we say that $F \subset \mathbb{R}^n$ is a negative feature of Ω if $\overline{F} \cap \overline{\Omega} \subset \partial\Omega$. In the following, we consider domains with arbitrary, but finite, numbers $N_f \in \mathbb{N}$ of negative features. We denote the set of all features by $\mathcal{F} = \{F^1, \dots, F^{N_f}\}$. Hereby, we assume that the features are *separated*. That is, we assume that

$$\overline{F}^k \cap \overline{F}^\ell = \emptyset \quad \forall k, \ell = 1, \dots, N_f, k \neq \ell.$$

The *defeatured domain* Ω_0 is then defined by

$$\Omega_0 := \Omega \cup \text{int} \left(\bigcup_{F \in \mathcal{F}} \overline{F} \right).$$

For a feature $F \in \mathcal{F}$, we define the *defeatured boundary* of the feature F , $\gamma^F := \text{int}(\overline{\partial\Omega} \cap \overline{\partial F})$. This is the piece of the boundary that is lost, when the feature F is removed from the geometry. In contrast, the *simplified boundary* of the feature is then defined as $\gamma_0^F := \partial F \setminus \gamma^F$. This is the piece of the defeatured boundary $\partial\Omega_0$ that is added, when the feature F is removed from the geometry; see Fig. 1. In particular, we have $\partial F = \overline{\gamma^F} \cup \overline{\gamma_0^F}$. The complete defeatured and simplified boundaries are, respectively, defined as

$$\gamma := \text{int} \left(\bigcup_{F \in \mathcal{F}} \overline{\gamma^F} \right), \quad \text{and} \quad \gamma_0 := \text{int} \left(\bigcup_{F \in \mathcal{F}} \overline{\gamma_0^F} \right).$$

Note that for an internal feature F , the simplified boundary γ_0^F is empty; see Fig. 1a.

2.2. Functional spaces and operators

Let $L^p(\omega)$ denote the standard Lebesgue spaces of exponent $p \in [1, \infty]$, equipped with the standard norm denoted by $\|\cdot\|_{L^p(\omega)}$. For a multi-index $\alpha \in \mathbb{N}_0^d$, we denote by D^α the partial derivative operator. We write $H^s(\omega)$ for the standard Sobolev

space of order $s \geq 0$, endowed with the standard norm $\|\cdot\|_{s,\omega}$; see e.g. Leoni.²⁴ Writing $|\alpha| := \sum_{i=1}^d \alpha_i$, the latter is defined by

$$\|v\|_{s,\omega}^2 := \|v\|_{[s],\omega}^2 + |v|_{\theta,\omega}^2, \quad \|v\|_{[s],\omega}^2 := \sum_{0 \leq |\alpha| \leq [s]} \|D^\alpha v\|_{0,\omega}^2, \quad (1)$$

$$|v|_{\theta,\omega}^2 := \sum_{|\alpha|=[s]} \int_\omega \int_\omega \frac{|D^\alpha v(x) - D^\alpha v(y)|^2}{|x-y|^{n+2\theta}} ds(x) ds(y), \quad (2)$$

where $s = [s] + \theta \geq 0$ and ds denotes the $(n-1)$ -dimensional Hausdorff measure if $d = n-1$ and the Lebesgue measure if $d = n$. The vector-valued Lebesgue and Sobolev spaces are denoted by $\mathbf{L}^2(\omega) = [L^2(\omega)]^n$ and $\mathbf{H}^s(\omega) = [H^s(\omega)]^n$, respectively. In addition, we define the average of a function over ω by

$$\bar{v}^\omega := \frac{1}{|\omega|} \int_\omega v(x) ds(x), \quad \forall v \in L^2(\omega).$$

For a subset Λ of the Lipschitz boundary $\partial\Omega$ with $|\Lambda| > 0$, we write $\tau_\Lambda : H^1(\Omega) \rightarrow H^{1/2}(\Lambda)$ and $R_\Lambda : H^{1/2}(\Lambda) \rightarrow H^1(\Omega)$ for the unique trace and corresponding lifting operator,²⁴ respectively, such that $\tau_\Lambda(R_\Lambda(\mu)) = \mu$ for all $\mu \in H^{1/2}(\Lambda)$. In particular, for a function $\mu \in H^{1/2}(\Lambda)$, we may define the subset

$$H_{\mu,\Lambda}^1(\Omega) := \{v \in H^1(\Omega) : \tau_\Lambda(v) = \mu\}.$$

Finally, we define the Neumann trace operator as the continuous linear operator $\nu_n : H(\text{div}; \Omega) \rightarrow H^{-1/2}(\partial\Omega)$, such that for $v \in H(\text{div}; \Omega)$ and $\mu \in H^{1/2}(\Omega)$,

$$\langle \nu_n(v), \mu \rangle := \int_\Omega v \cdot \nabla R_{\partial\Omega}(\mu) dx + \int_\Omega \text{div}(v) R_{\partial\Omega}(\mu) dx, \quad (3)$$

where $\langle \cdot, \cdot \rangle$ denotes the duality pairing between $H^{1/2}(\partial\Omega)$ and $H^{-1/2}(\partial\Omega)$. In particular, for $w \in H^{3/2}(\Omega)$ such that $\Delta w \in L^2(\Omega)$, it holds that $\nu_n(\nabla w) \in L^2(\partial\Omega)$.²⁷

2.3. Linear quantities of interest

Let us now abstractly introduce linear QoIs, in terms of which we later want to quantify the defeathering error. To that end, let $V(\Omega)$ and $V_0(\Omega_0)$ be Hilbert spaces over the exact domain Ω and defeatured domain Ω_0 , respectively. Then, a linear QoI is given by a linear functional L in the dual space $V(\Omega)'$. We denote by $L_0 \in V_0(\Omega_0)'$ the defeatured counterpart of L , whereby we make the following assumption:

Assumption 2.1. *The defeatured QoI L_0 satisfies*

$$L_0(v_0) = L((v_0)_{|\Omega}) \quad \forall v_0 \in V_0.$$

Assumption 2.1 serves as a simplifying assumption in this paper. It expresses that neither L nor L_0 interacts with the feature and its boundary, which holds for any localized QoI, but not for global ones such as the compliance.

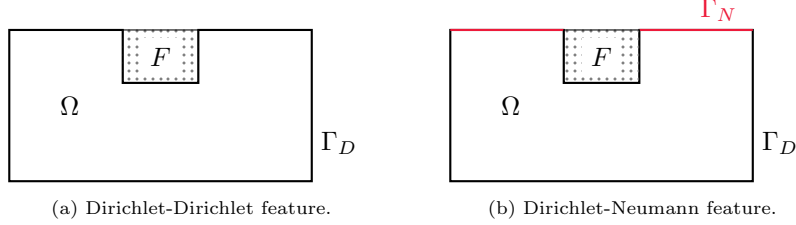


Fig. 2: Illustration of the two types of Dirichlet boundary features: (a) Dirichlet-Dirichlet feature and (b) Dirichlet-Neumann feature.

3. Defeaturing Poisson's equation

Poisson's equation provides the simplest setting to develop and illustrate the central ideas of our goal-oriented defeaturing framework. This model problem allows us to introduce the classification of features, formulate the defeaturing problem for geometries with multiple Dirichlet and Neumann features, and establish both energy-norm and goal-oriented error estimators. The arguments presented here form the blueprint for the subsequent extensions to linear elasticity and Stokes flow.

To that end, we decompose the set of features \mathcal{F} from section 2.1 into the sets of Dirichlet features \mathcal{F}_D and Neumann features \mathcal{F}_N , respectively such that $\mathcal{F} = \mathcal{F}_D \cup \mathcal{F}_N$. For technical reasons, we must distinguish between three different types within the Dirichlet features: First, *internal* features that are not in contact with any other boundaries, denoted by $\mathcal{F}_{D,\text{int}} \subset \mathcal{F}_D$; second, *Dirichlet-Dirichlet* features, that only touch other Dirichlet boundaries, denoted by $\mathcal{F}_{DD} \subset \mathcal{F}_D$; and third, *Dirichlet-Neumann* features that may also touch other Neumann boundaries, which we denote by $\mathcal{F}_{DN} \subset \mathcal{F}_D$. We refer to Weder and Buffa³⁸ for an in-depth discussion of this distinction.

The two different Dirichlet boundary feature types are illustrated in Fig. 2. In contrast, no such distinction is necessary for Neumann features.¹⁰ Moreover, we can decompose the complete defeatured and simplified boundaries as

$$\gamma = \text{int}(\overline{\gamma_D} \cup \overline{\gamma_N}), \quad \text{and} \quad \gamma_0 = \text{int}(\overline{\gamma_{0,D}} \cup \overline{\gamma_{0,N}}),$$

where the Dirichlet pieces are defined by

$$\gamma_D := \text{int} \left(\bigcup_{F \in \mathcal{F}_D} \overline{\gamma^F} \right), \quad \text{and} \quad \gamma_{0,D} := \text{int} \left(\bigcup_{F \in \mathcal{F}_{DD} \cup \mathcal{F}_{D,\text{int}}} \overline{\gamma_0^F} \right),$$

while the Neumann pieces are defined by

$$\gamma_N := \text{int} \left(\bigcup_{F \in \mathcal{F}_N} \overline{\gamma^F} \right), \quad \text{and} \quad \gamma_{0,N} := \text{int} \left(\bigcup_{F \in \mathcal{F}_N \cup \mathcal{F}_{DN}} \overline{\gamma_0^F} \right).$$

Remark 3.1. *On simplified boundaries of Dirichlet-Neumann features, we intentionally impose Neumann conditions to avoid tracking complex intersections with*

surrounding boundaries. However, in terms of the analysis, one could also impose Dirichlet data.

To formulate the problem in the exact domain Ω , its boundary $\partial\Omega$ is decomposed into the Dirichlet and Neumann parts, i.e. $\partial\Omega = \Gamma_D \cup \Gamma_N$, where $\Gamma_D \cap \Gamma_N = \emptyset$. Particularly, we have $\gamma_D \subset \Gamma_D$ and $\gamma_N \subset \Gamma_N$. Then, the exact problem reads

$$\begin{cases} -\Delta u = f & \text{in } \Omega, \\ u = g & \text{on } \Gamma_D, \\ \partial_n u = h & \text{on } \Gamma_N, \end{cases} \quad (4)$$

for boundary data $g \in H^{1/2}(\Gamma_D)$ and $h \in L^2(\Gamma_N)$ and a source term $f \in L^2(\Omega)$. Problem (4) is well-posed in $V(\Omega) = H_{g,\Gamma_D}^1(\Omega)$, even with slightly weaker regularity assumptions, but we assume the latter for simplicity.¹¹

Similarly, we can decompose the boundary of the defeatured domain as $\partial\Omega_0 = \Gamma_{D,0} \cup \Gamma_{0,N}$. After choosing suitable extensions of the boundary data $g_0 \in H^{1/2}(\Gamma_{0,D})$ and $h_0 \in L^2(\Gamma_{0,N})$, the defeatured problem reads

$$\begin{cases} -\Delta u_0 = f & \text{in } \Omega_0, \\ u_0 = g_0 & \text{on } \Gamma_{0,D}, \\ \partial_n u_0 = h_0 & \text{on } \Gamma_{0,N}, \end{cases} \quad (5)$$

where we write f for an L^2 -extension of the source term in Ω to Ω_0 by abuse of notation. Problem (5) is also well-posed in $V_0(\Omega) = H_{g_0,\Gamma_{0,D}}^1(\Omega_0)$. Having set up the defeaturing problem for Poisson's equation, we now turn to quantifying the error between u and u_0 in the corresponding energy norm.

3.1. Energy-norm estimates

In this subsection, we establish energy-norm estimates that quantify the error introduced by defeaturing in the Poisson problem. For ease of notation, we define the defeaturing error function $e := u - (u_0)_{|\Omega}$, which satisfies the PDE

$$\begin{cases} -\Delta e = 0 & \text{in } \Omega, \\ e = 0 & \text{on } \Gamma_D \setminus \overline{\gamma_D}, \\ e = d_{\gamma_D} & \text{on } \gamma_D, \\ \partial_n e = 0 & \text{on } \Gamma_N \setminus \overline{\gamma_N}, \\ \partial_n e = d_{\gamma_N} & \text{on } \gamma_N, \end{cases} \quad (6)$$

where $d_{\gamma_D} := g|_{\gamma_D} - (u_0)|_{\gamma_D}$ and $d_{\gamma_N} := h|_{\gamma_N} - (\partial_n u_0)|_{\gamma_N}$. For the individual features, we similarly define the boundary errors by

$$d_{\gamma^F} := \begin{cases} g|_{\gamma^F} - (u_0)|_{\gamma^F} & F \in \mathcal{F}_D, \\ h|_{\gamma^F} - (\partial_n u_0)|_{\gamma^F} & F \in \mathcal{F}_N. \end{cases}$$

Note that in general, the defeaturing error e belongs to $H^1(\Omega)$. While the following analysis can be conducted under minimal regularity assumptions following the argument presented by Weder and Buffa,³⁸ we assume for ease of exposition that $e \in H^{3/2}(\Omega)$. This assumption holds in Lipschitz domains under light assumptions on the problem data and the interfaces between Dirichlet and Neumann boundaries.¹⁹ This regularity assumption implies that $\nu_n(\nabla e) \in L^2(\partial\Omega)$, which greatly simplifies the treatment of Dirichlet-Neumann features.

Recall that the energy norm associated with the Poisson problem is given by the H^1 -seminorm, i.e., $\|v\|_\Omega := |v|_{1,\Omega}$ for $v \in H_{\Omega,0}^1(\Gamma_D)$. Using integration by parts and (6), we find similarly to Buffa et al.⁷ and Weder and Buffa³⁸ that

$$\begin{aligned} |e|_{1,\Omega}^2 &= \int_{\partial\Omega} \partial_n e \, e \, ds \\ &= \sum_{F \in \mathcal{F}_{DD}} \int_{\gamma^F} \nu_n(\nabla e) d_{\gamma^F} \, ds + \sum_{F \in \mathcal{F}_{D,int}} \int_{\gamma^F} \nu_n(\nabla e) d_{\gamma^F} \, ds \\ &\quad + \sum_{F \in \mathcal{F}_{DN}} \int_{\gamma^F} \nu_n(\nabla e) d_{\gamma^F} \, ds + \sum_{F \in \mathcal{F}_N} \int_{\gamma^F} d_{\gamma^F} e|_{\gamma^F} \, ds. \end{aligned} \quad (7)$$

To derive an estimator expression from (7), we follow the arguments of Buffa and Chanon⁷ and Weder and Buffa.³⁸ That is, for the integrals in the four sums of (7), we seek estimates of the form

$$\int_{\gamma^F} \nu_n(\nabla e) d_{\gamma^F} \, ds \lesssim \mathcal{E}^{\gamma^F}(u_0) |e|_{1,\Omega}, \quad \text{or} \quad \int_{\gamma^F} d_{\gamma^F} e|_{\gamma^F} \, ds \lesssim \mathcal{E}^{\gamma^F}(u_0) |e|_{1,\Omega},$$

for Dirichlet features $F \in \mathcal{F}_D$ and Neumann features $F \in \mathcal{F}_N$, respectively. Here, $\mathcal{E}^{\gamma^F}(u_0)$ denotes a generic estimator expression, whose structure depends on the specific feature type.

Indeed, applying the Cauchy-Schwarz inequality separates the unknown error terms $\nu_n(\nabla e)$ or $e|_{\gamma^F}$ from the boundary errors d_{γ^F} . The subsequent bounds rely on Poincaré-type inequalities on the boundary γ^F , the choice of which depends on the behavior of d_{γ^F} at the intersection with the remaining boundary: For a Dirichlet-Dirichlet feature, the boundary error d_{γ^F} vanishes at the boundary of the feature and the classical Poincaré inequality applies (Lemma A.1). For a Dirichlet-Neumann feature, the boundary error does not vanish at the boundary of the feature anymore. Hence, the average must be removed before a Poincaré inequality can be applied (Lemma A.2). Similar issues arise for internal Dirichlet and Neumann features. For the details, we refer to Buffa et al.⁷ and Weder and Buffa.³⁸

The following estimator expressions are shown to be reliable for the different

feature types in Refs. 7 and 38, respectively:

$$\begin{aligned}\mathcal{E}_N^{\gamma^F}(u_0) &:= \left(|\gamma^F|^{\frac{1}{n-1}} \|d_{\gamma^F} - \overline{d_{\gamma^F}}^{\gamma^F}\|_{0,\gamma^F}^2 + c_{\gamma^F}^2 |\gamma^F|^{\frac{n}{n-1}} |\overline{d_{\gamma^F}}^{\gamma^F}|^2 \right)^{\frac{1}{2}}, \\ \mathcal{E}_{DD}^{\gamma^F}(u_0) &:= \sqrt{2 \|d_{\gamma^F}\|_{0,\gamma^F} \|\nabla_t d_{\gamma^F}\|_{0,\gamma^F}}, \\ \mathcal{E}_{DN}^{\gamma^F}(u_0) &:= \sqrt{2 \|d_{\gamma^F} - \overline{d_{\gamma^F}}^{\gamma^F}\|_{0,\gamma^F} \|\nabla_t d_{\gamma^F}\|_{0,\gamma^F} + |\gamma^F|^{\frac{n-2}{2(n-1)}} |\overline{d_{\gamma^F}}^{\gamma^F}|}, \\ \mathcal{E}_{int}^{\gamma^F}(u_0) &:= 2 \sqrt{\|d_{\gamma^F} - \overline{d_{\gamma^F}}^{\gamma^F}\|_{0,\gamma^F} \|\nabla_t d_{\gamma^F}\|_{0,\gamma^F} + \bar{c}_{\gamma^F} |\overline{d_{\gamma^F}}^{\gamma^F}|}.\end{aligned}$$

Here, $\nabla_t d_{\gamma^F}$ denotes the tangential gradient along γ^F . The constant c_{γ^F} is defined by

$$c_{\gamma^F} := \begin{cases} \max(-\log(|\gamma^F|), \eta)^{\frac{1}{2}} & \text{if } n = 2, \\ 1 & \text{if } n = 3, \end{cases}$$

where $\eta \in \mathbb{R}$ is the unique solution to $\eta = -\log(\eta)$; see [Ref. 7, p. 8]. The constant \bar{c}_{γ^F} is defined by

$$\bar{c}_{\gamma^F} := \begin{cases} \sqrt{\frac{2\pi}{|\log(s_{\gamma^F})|}}, & n = 2, \\ \sqrt{\frac{2\pi \operatorname{diam}(\gamma^F)}{1-s_{\gamma^F}}}, & n = 3 \end{cases}, \quad \text{where} \quad s_{\gamma^F} := \frac{\operatorname{diam}(\gamma^F)}{2 \operatorname{dist}(m_F, \partial\Omega \setminus \overline{\gamma^F})},$$

and m_F denotes the barycenter of the feature F ; see Lemma 4.3 in Weder and Buffa.³⁸

Adding up the feature-wise contributions, we then find the global estimate

$$\begin{aligned}|e|_{1,\Omega}^2 &\lesssim |e|_{1,\Omega} \left(\sum_{F \in \mathcal{F}_{DD}} \mathcal{E}_{DD}^{\gamma^F}(u_0)^2 + \sum_{F \in \mathcal{F}_{D,int}} \mathcal{E}_{int}^{\gamma^F}(u_0)^2 \right. \\ &\quad \left. + \sum_{F \in \mathcal{F}_{DN}} \mathcal{E}_{DN}^{\gamma^F}(u_0)^2 + \sum_{F \in \mathcal{F}_N} \mathcal{E}_N^{\gamma^F}(u_0)^2 \right)^{\frac{1}{2}}.\end{aligned}$$

Hence, we define the general multi-feature estimator by

$$\begin{aligned}\mathcal{E}_{\mathcal{F}}^{\gamma}(u_0) &:= \left(\sum_{F \in \mathcal{F}_{DD}} \mathcal{E}_{DD}^{\gamma^F}(u_0)^2 + \sum_{F \in \mathcal{F}_{D,int}} \mathcal{E}_{int}^{\gamma^F}(u_0)^2 \right. \\ &\quad \left. + \sum_{F \in \mathcal{F}_{DN}} \mathcal{E}_{DN}^{\gamma^F}(u_0)^2 + \sum_{F \in \mathcal{F}_N} \mathcal{E}_N^{\gamma^F}(u_0)^2 \right)^{\frac{1}{2}},\end{aligned}\tag{8}$$

whose reliability immediately follows from the reliability of the feature-wise estimators.

3.2. Goal-oriented estimates

We now turn to the derivation of goal-oriented estimates for the Poisson problem defined above. To this end, let $L \in V(\Omega)'$ be a linear QoI as defined in section 2.3 with a defeatured counterpart $L_0 \in V_0(\Omega_0)'$ satisfying Assumption 2.1. Motivated by the dual-weighted residual method,⁴ we represent L and L_0 with the help of influence functions z and z_0 , solving the following dual problems, respectively:

$$\begin{cases} -\Delta z = L & \text{in } \Omega, \\ z = 0 & \text{on } \Gamma_D, \\ \partial_n z = 0 & \text{on } \Gamma_N, \end{cases} \quad \text{and} \quad \begin{cases} -\Delta z_0 = L_0 & \text{in } \Omega_0, \\ z_0 = 0 & \text{on } \Gamma_{0,D}, \\ \partial_n z_0 = 0 & \text{on } \Gamma_{0,N}. \end{cases} \quad (9)$$

For the well-posedness of these problems, we refer to Agranovich.¹ In addition, the energy-based estimate from the previous section still holds. The dual defeaturing error $\epsilon := z - (z_0)|_{\Omega}$ immediately satisfies the estimate $|\epsilon|_{1,\Omega} \lesssim \mathcal{E}_{\mathcal{F}}^{\gamma}(z_0)$.

To derive a goal-oriented estimate, we first note that in virtue of Assumption 2.1, we have

$$L(u) - L_0(u_0) = L(u) - L((u_0)|_{\Omega}) = L(\epsilon).$$

Next, using the error PDE (6) for the primal error e and the exact dual problem, we obtain from two successive integrations by parts that

$$\begin{aligned} L(\epsilon) &= \int_{\Omega} (-\Delta z) e \, dx = \int_{\Omega} \nabla z \cdot \nabla e \, dx - \int_{\partial\Omega} \nu_n(\nabla z) e \, ds \\ &= \int_{\partial\Omega} \nu_n(\nabla e) z \, ds - \int_{\partial\Omega} \nu_n(\nabla z) e \, ds. \end{aligned}$$

Using the boundary conditions of the exact dual problem in (9), we find an error representation similar to (7):

$$\begin{aligned} L(\epsilon) &= \sum_{F \in \mathcal{F}_N} \int_{\gamma^F} d_{\gamma^F} z|_{\gamma^F} \, ds - \sum_{F \in \mathcal{F}_{DD}} \int_{\gamma^F} \nu_n(\nabla z) d_{\gamma^F} \, ds \\ &\quad - \sum_{F \in \mathcal{F}_{D,int}} \int_{\gamma^F} \nu_n(\nabla z) d_{\gamma^F} \, ds - \sum_{F \in \mathcal{F}_{DN}} \int_{\gamma^F} \nu_n(\nabla z) d_{\gamma^F} \, ds. \end{aligned} \quad (10)$$

Note, however, that (10) still involves the exact dual solution z . The idea is now to split the right-hand side of (10) into a term that only involves the defeatured solutions u_0 and z_0 and a term that only involves the error functions e and ϵ . To that purpose, we define the corrector term

$$\begin{aligned} R_L^{\gamma}(u_0, z_0) &:= \sum_{F \in \mathcal{F}_N} \int_{\gamma^F} d_{\gamma^F} (z_0)|_{\gamma^F} \, ds - \sum_{F \in \mathcal{F}_{DD}} \int_{\gamma^F} \nu_n(\nabla z_0) d_{\gamma^F} \, ds \\ &\quad - \sum_{F \in \mathcal{F}_{D,int}} \int_{\gamma^F} \nu_n(\nabla z_0) d_{\gamma^F} \, ds - \sum_{F \in \mathcal{F}_{DN}} \int_{\gamma^F} \nu_n(\nabla z_0) d_{\gamma^F} \, ds. \end{aligned} \quad (11)$$

With this corrector at hand, we can prove the following result:

Theorem 3.2. *Let Ω be a Lipschitz domain with a set of negative isotropic Lipschitz features \mathcal{F} . Let $L \in V(\Omega)'$ and $L_0 \in V_0(\Omega)'$ be linear QoIs such that Assumption 2.1 is satisfied. Furthermore, let u and u_0 be the solutions to the exact problem (4) and defeatured problem (5), respectively, and z_0 the solution to the defeatured dual problem (9). Then, the following estimate holds:*

$$|L(u) - L_0(u_0) - R_L^\gamma(u_0, z_0)| \lesssim \mathcal{E}_{\mathcal{F}}^\gamma(u_0) \mathcal{E}_{\mathcal{F}}^\gamma(z_0).$$

Proof. Using the error representation (10) and the corrector term from (11), we obtain

$$\begin{aligned} L(e) - R_L^\gamma(u_0, z_0) &= \sum_{F \in \mathcal{F}_N} \int_{\gamma^F} d_{\gamma^F} \epsilon|_{\gamma^F} \, ds - \sum_{F \in \mathcal{F}_{DD}} \int_{\gamma^F} \nu_n(\nabla \epsilon) \, d_{\gamma^F} \, ds \\ &\quad - \sum_{F \in \mathcal{F}_{D,int}} \int_{\gamma^F} \nu_n(\nabla \epsilon) \, d_{\gamma^F} \, ds - \sum_{F \in \mathcal{F}_{DN}} \int_{\gamma^F} \nu_n(\nabla \epsilon) \, d_{\gamma^F} \, ds. \end{aligned}$$

Now, observe that the integrals in the sums above have the same structure as the ones in (10). Hence, with the same arguments from Buffa et al.⁷ and Weder and Buffa,³⁸ we find

$$\begin{aligned} |L(e) - R_L^\gamma(u_0, z_0)| &\lesssim |\epsilon|_{1,\Omega} \left(\sum_{F \in \mathcal{F}_N} \mathcal{E}_N^{\gamma^F}(u_0)^2 + \sum_{F \in \mathcal{F}_{DD}} \mathcal{E}_{DD}^{\gamma^F}(u_0)^2 \right. \\ &\quad \left. + \sum_{F \in \mathcal{F}_{D,int}} \mathcal{E}_{D,int}^{\gamma^F}(u_0)^2 + \sum_{F \in \mathcal{F}_{DN}} \mathcal{E}_{DN}^{\gamma^F}(u_0)^2 \right)^{\frac{1}{2}} \lesssim \mathcal{E}_{\mathcal{F}}^\gamma(u_0) \mathcal{E}_{\mathcal{F}}^\gamma(z_0). \end{aligned}$$

□

Remark 3.3. *In light of Theorem 3.2, we observe that apart from ensuring the reliability of the goal-oriented estimate, the correction term $R_L^\gamma(u_0, z_0)$ provides a first-order correction of the defeatured QoI $L_0(u_0)$. That is, if the product $\mathcal{E}_{\mathcal{F}}^\gamma(u_0) \mathcal{E}_{\mathcal{F}}^\gamma(z_0)$ is small enough, the estimate implies that the approximation*

$$L(u) \approx L_0(u_0) + R_L^\gamma(u_0, z_0),$$

is accurate. We will refer to the right-hand side as the corrected QoI.

The same structure now naturally extends to the linear elasticity and Stokes' equations.

4. Defeaturing the linear elasticity equation

In this section, we present the general defeaturing problem for the linear elasticity equations for mixed negative Dirichlet and Neumann features. It closely follows section 3, Antolín and Chanon² and Chanon,¹⁰ where the case of Neumann features was addressed.

For a function $\mathbf{v} : \Omega \rightarrow \mathbb{R}^n$, we define the *linearized strain rate tensor* and the *Cauchy stress tensor*, respectively, by

$$\mathbb{E}(\mathbf{v}) := \frac{1}{2}(\nabla \mathbf{v} + \nabla \mathbf{v}^\top), \quad \text{and} \quad \mathbb{S}(\mathbf{v}) := 2\mu \mathbb{E}(\mathbf{v}) + \lambda(\nabla \cdot \mathbf{v})\mathbb{I}_n,$$

where μ and λ denote the Lamé constants. We recall that due to thermodynamic stability, $\mu > 0$ and $\lambda + \frac{2}{3}\mu > 0$. Let $\mathbf{g} \in \mathbf{H}^{1/2}(\Gamma_D)$, $\mathbf{h} \in \mathbf{L}^2(\Gamma_N)$, and $\mathbf{f} \in \mathbf{L}^2(\Omega)$. Then the linear elasticity equations in the exact domain read:

$$\begin{cases} -\nabla \cdot \mathbb{S}(\mathbf{u}) = \mathbf{f} & \text{in } \Omega, \\ \mathbf{u} = \mathbf{g} & \text{on } \Gamma_D, \\ \mathbb{S}(\mathbf{u})\mathbf{n} = \mathbf{h} & \text{on } \Gamma_N, \end{cases} \quad (12)$$

where \mathbf{n} denotes the unitary outward normal of $\partial\Omega$. The corresponding weak formulation reads: Find $\mathbf{u} \in V(\Omega) := \mathbf{H}_{\mathbf{g}, \Gamma_D}^1(\Omega)$, such that for all $\mathbf{v} \in \mathbf{H}_{0, \Gamma_D}^1(\Omega)$,

$$\int_{\Omega} \mathbb{S}(\mathbf{u}) : \mathbb{E}(\mathbf{v}) \, dx = \int_{\Omega} \mathbf{f} \cdot \mathbf{v} \, dx + \int_{\Gamma_N} \mathbf{h} \cdot \mathbf{v} \, ds. \quad (13)$$

The energy norm corresponding to problem (13) is defined by

$$\|\mathbf{v}\|_{\Omega} := \left(\int_{\Omega} \mathbb{S}(\mathbf{v}) : \mathbb{E}(\mathbf{v}) \, dx \right)^{\frac{1}{2}}, \quad \forall \mathbf{v} \in V(\Omega).$$

For the defeatured domain Ω_0 , we write \mathbf{f} for an L^2 -extension of the source term in (12) by abuse of notation. Once we have chosen extensions $\mathbf{g}_0 \in \mathbf{H}^{1/2}(\Gamma_{0,D})$ and $\mathbf{h}_0 \in \mathbf{L}^2(\Gamma_{0,N})$ of \mathbf{g} and \mathbf{h} , respectively, the defeatured elasticity problem reads:

$$\begin{cases} -\nabla \cdot \mathbb{S}(\mathbf{u}_0) = \mathbf{f} & \text{in } \Omega_0, \\ \mathbf{u}_0 = \mathbf{g}_0 & \text{on } \Gamma_{0,D}, \\ \mathbb{S}(\mathbf{u}_0)\mathbf{n} = \mathbf{h}_0 & \text{on } \Gamma_{0,N}. \end{cases} \quad (14)$$

The exact problem (12) and its defeatured counterpart (14) are well-posed in $V(\Omega)$ and $V_0(\Omega_0) := \mathbf{H}_{\mathbf{g}_0, \Gamma_{0,D}}^1(\Omega_0)$, respectively.

Similar to the Poisson problem, we define the vector-valued defeaturing error $\mathbf{e} := \mathbf{u} - (\mathbf{u}_0)_{|\Omega}$. For each feature F , we introduce the boundary error as

$$\mathbf{d}_{\gamma^F} := \begin{cases} \mathbf{g}_{|\gamma^F} - (\mathbf{u}_0)_{|\gamma^F}, & F \in \mathcal{F}_D, \\ \mathbf{h}_{|\gamma^F} - \mathbb{S}(\mathbf{u}_0)\mathbf{n}_{|\gamma^F}, & F \in \mathcal{F}_N. \end{cases}$$

Analogously to the Poisson case in section 3, an integration by parts argument yields a general boundary error representation for the elasticity problem:

$$\begin{aligned} \|\mathbf{e}\|_{\Omega}^2 &= \sum_{F \in \mathcal{F}_{DD}} \int_{\gamma^F} (\mathbb{S}(\mathbf{e})\mathbf{n}) \cdot \mathbf{d}_{\gamma^F} \, ds + \sum_{F \in \mathcal{F}_{D,\text{int}}} \int_{\gamma^F} (\mathbb{S}(\mathbf{e})\mathbf{n}) \cdot \mathbf{d}_{\gamma^F} \, ds \\ &\quad + \sum_{F \in \mathcal{F}_{DN}} \int_{\gamma^F} (\mathbb{S}(\mathbf{e})\mathbf{n}) \cdot \mathbf{d}_{\gamma^F} \, ds + \sum_{F \in \mathcal{F}_N} \int_{\gamma^F} \mathbf{d}_{\gamma^F} \cdot \mathbf{e}_{|\gamma^F} \, ds. \end{aligned} \quad (15)$$

Here we make the same regularity assumption that $\mathbf{s}(\mathbf{e})\mathbf{n} \in \mathbf{L}^2(\partial\Omega)$ as for the Poisson problem for simplicity. However, the analysis can be conducted under minimal regularity assumptions; see Appendix B. The boundary representation (15) naturally suggests the following computable multi-feature estimator:

$$\begin{aligned} \mathcal{E}_{\mathcal{F}}^{\gamma}(\mathbf{u}_0) &:= \left(\sum_{F \in \mathcal{F}_{DD}} \mathcal{E}_{DD}^{\gamma^F}(\mathbf{u}_0)^2 + \sum_{F \in \mathcal{F}_{D,int}} \mathcal{E}_{int}^{\gamma^F}(\mathbf{u}_0)^2 \right. \\ &\quad \left. + \sum_{F \in \mathcal{F}_{DN}} \mathcal{E}_{DN}^{\gamma^F}(\mathbf{u}_0)^2 + \sum_{F \in \mathcal{F}_N} \mathcal{E}_N^{\gamma^F}(\mathbf{u}_0)^2 \right)^{\frac{1}{2}}, \end{aligned} \quad (16)$$

with the feature-wise estimators given by

$$\mathcal{E}_N^{\gamma^F}(\mathbf{u}_0) := \left(|\gamma^F|^{\frac{1}{n-1}} \|\mathbf{d}_{\gamma^F} - \overline{\mathbf{d}_{\gamma^F}}^{\gamma^F}\|_{0,\gamma^F}^2 + c_{\gamma^F}^2 |\gamma^F|^{\frac{n}{n-1}} \|\overline{\mathbf{d}_{\gamma^F}}^{\gamma^F}\|_{\ell^2}^2 \right)^{\frac{1}{2}}, \quad (17)$$

$$\mathcal{E}_{DD}^{\gamma^F}(\mathbf{u}_0) := 2\sqrt{\|\mathbf{d}_{\gamma^F}\|_{0,\gamma^F} \|\nabla_t \mathbf{d}_{\gamma^F}\|_{0,\gamma^F}}, \quad (18)$$

$$\mathcal{E}_{DN}^{\gamma^F}(\mathbf{u}_0) := 2\sqrt{\|\mathbf{d}_{\gamma^F} - \overline{\mathbf{d}_{\gamma^F}}^{\gamma^F}\|_{0,\gamma^F} \|\nabla_t \mathbf{d}_{\gamma^F}\|_{0,\gamma^F} + 2|\gamma^F|^{\frac{n-2}{2(n-1)}} \|\overline{\mathbf{d}_{\gamma^F}}^{\gamma^F}\|_{\ell^2}}, \quad (19)$$

$$\mathcal{E}_{int}^{\gamma^F}(\mathbf{u}_0) := 2\sqrt{\|\mathbf{d}_{\gamma^F} - \overline{\mathbf{d}_{\gamma^F}}^{\gamma^F}\|_{0,\gamma^F} \|\nabla_t \mathbf{d}_{\gamma^F}\|_{0,\gamma^F} + \bar{c}_{\gamma^F} \|\overline{\mathbf{d}_{\gamma^F}}^{\gamma^F}\|_{\ell^2}}. \quad (20)$$

The reliability of (17) for a Neumann feature was shown by Antolín and Chanon.² For the proof of reliability of the estimators for Dirichlet features (18) to (20), we refer to Theorem B.2 in Appendix B. The feature-wise reliability of the estimators thus implies that $\|\mathbf{e}\|_{\Omega} \lesssim \mathcal{E}_{\mathcal{F}}^{\gamma}(\mathbf{u}_0)$ like in the case of the Poisson problem.

Consider now a linear QoI $L \in V(\Omega)'$ and a corresponding defeatured QoI $L_0 \in V_0(\Omega)'$ satisfying Assumption 2.1. Then, similar to the Poisson problem in section 3, we define the exact and defeatured dual problems,

$$\begin{cases} -\nabla \cdot \mathbf{s}(\mathbf{z}) = L & \text{in } \Omega, \\ \mathbf{z} = \mathbf{0} & \text{on } \Gamma_D, \\ \mathbf{s}(\mathbf{z})\mathbf{n} = \mathbf{0} & \text{on } \Gamma_N, \end{cases} \quad \text{and} \quad \begin{cases} -\nabla \cdot \mathbf{s}(\mathbf{z}_0) = L_0 & \text{in } \Omega_0, \\ \mathbf{z}_0 = \mathbf{0} & \text{on } \Gamma_{0,D}, \\ \mathbf{s}(\mathbf{z}_0)\mathbf{n} = \mathbf{0} & \text{on } \Gamma_{0,N}. \end{cases} \quad (21)$$

For the dual defeaturing error $\mathbf{\epsilon} := \mathbf{z} - (\mathbf{z}_0)_{\Omega}$, the energy-norm estimate $\|\mathbf{\epsilon}\|_{\Omega} \lesssim \mathcal{E}_{\mathcal{F}}^{\gamma}(\mathbf{z}_0)$ also holds.

In analogy to the corrector term (11) for the Poisson problem, we define

$$\begin{aligned} R_L^{\gamma}(\mathbf{u}_0, \mathbf{z}_0) &:= \sum_{F \in \mathcal{F}_N} \int_{\gamma^F} \mathbf{d}_{\gamma^F} \cdot (\mathbf{z}_0)_{|\gamma^F} \, ds - \sum_{F \in \mathcal{F}_{DD}} \int_{\gamma^F} (\mathbf{s}(\mathbf{z}_0)\mathbf{n}) \cdot \mathbf{d}_{\gamma^F} \, ds \\ &\quad - \sum_{F \in \mathcal{F}_{D,int}} \int_{\gamma^F} (\mathbf{s}(\mathbf{z}_0)\mathbf{n}) \cdot \mathbf{d}_{\gamma^F} \, ds - \sum_{F \in \mathcal{F}_{DN}} \int_{\gamma^F} (\mathbf{s}(\mathbf{z}_0)\mathbf{n}) \cdot \mathbf{d}_{\gamma^F} \, ds. \end{aligned}$$

Then, the same reasoning as for the Poisson equation yields the following result:

Theorem 4.1. *Let Ω be a Lipschitz domain with a set of negative isotropic Lipschitz features \mathcal{F} . Let $L \in V(\Omega)'$ and $L_0 \in V_0(\Omega)'$ be linear QoIs such that Assumption 2.1 is satisfied. Furthermore, let \mathbf{u} and \mathbf{u}_0 be the solutions to the exact problem (12) and defeatured problem (14), respectively, and \mathbf{z}_0 the solution to the defeatured dual problem (21). Then, the following estimate holds:*

$$|L(\mathbf{u}) - L_0(\mathbf{u}_0) - R_L^\gamma(\mathbf{u}_0, \mathbf{z}_0)| \lesssim \mathcal{E}_{\mathcal{F}}^\gamma(\mathbf{u}_0) \mathcal{E}_{\mathcal{F}}^\gamma(\mathbf{z}_0).$$

5. Defeaturing the Stokes equations

This section addresses the general defeaturing problem for the Stokes equations for mixed negative Dirichlet and Neumann features. It closely follows sections 3 and 4.

To that end, let $\mathbf{e}(\mathbf{v})$ denote again the linearized strain rate tensor for a function $\mathbf{v} : \Omega \rightarrow \mathbb{R}^n$. In contrast to section 4, we denote by $\mathbf{s}(\mathbf{v})$ be the viscous stress tensor of the fluid, which for a Newtonian fluid is given by

$$\mathbf{s}(\mathbf{v}) = 2\mu\mathbf{e}(\mathbf{v}) + \lambda(\nabla \cdot \mathbf{v})\mathbb{I}_n,$$

with this time the constants $\mu > 0$ and $\lambda \geq 0$ denoting the bulk and dynamic viscosities, respectively. Let $\mathbf{g} \in \mathbf{H}^{1/2}(\Gamma_D)$, $\mathbf{h} \in \mathbf{L}^2(\Gamma_N)$, $\mathbf{f} \in \mathbf{L}^2(\Omega)$, and $f_c \in L^2(\Omega)$. Then, the Stokes problem in the exact domain is given by

$$\begin{cases} -\nabla \cdot \mathbf{s}(\mathbf{u}) + \nabla p = \mathbf{f} & \text{in } \Omega, \\ \nabla \cdot \mathbf{u} = f_c & \text{in } \Omega, \\ \mathbf{u} = \mathbf{g} & \text{on } \Gamma_D, \\ \mathbf{s}(\mathbf{u})\mathbf{n} - p\mathbf{n} = \mathbf{h} & \text{on } \Gamma_N, \end{cases} \quad (22)$$

where \mathbf{n} denotes the unitary outward normal of $\partial\Omega$. The corresponding mixed weak formulation reads: Find $\mathbf{u} \in V(\Omega) := \mathbf{H}_{\mathbf{g}, \Gamma_D}^1(\Omega)$ and $p \in Q(\Omega) := L^2(\Omega)$, such that for all $\mathbf{v} \in \mathbf{H}_{\mathbf{0}, \Gamma_D}^1(\Omega)$ and $q \in L^2(\Omega)$,

$$a_\Omega(\mathbf{u}, \mathbf{v}) + b_\Omega(\mathbf{v}, p) = \int_\Omega \mathbf{f} \cdot \mathbf{v} \, dx + \int_\Omega \mathbf{g}_N \cdot \mathbf{v} \, ds, \quad (23)$$

$$b_\Omega(\mathbf{u}, q) = - \int_\Omega f_c q \, dx, \quad (24)$$

where the bilinear forms $a_\Omega : \mathbf{H}^1(\Omega) \times \mathbf{H}^1(\Omega) \rightarrow \mathbb{R}$ and $b_\Omega : \mathbf{H}^1(\Omega) \times L^2(\Omega) \rightarrow \mathbb{R}$ are given by

$$a_\Omega(\mathbf{u}, \mathbf{v}) := \int_\Omega \mathbf{s}(\mathbf{u}) : \mathbf{e}(\mathbf{v}) \, dx, \quad \text{and} \quad b_\Omega(\mathbf{v}, q) := - \int_\Omega \nabla \cdot \mathbf{v} q \, dx.$$

This problem is well-posed in $V(\Omega) \times Q(\Omega)$; see Boffi et al.⁵ The energy norm associated with the weak formulation (23) and (24) is given by

$$\|(\mathbf{v}, q)\|_\Omega := a_\Omega(\mathbf{v}, \mathbf{v})^{\frac{1}{2}} + \|q\|_{0, \Omega}, \quad \forall \mathbf{v} \in \mathbf{H}^1(\Omega), q \in L^2(\Omega).$$

For the defeatured domain Ω_0 , we write \mathbf{f} and f_c for L^2 -extensions of the original source terms in (22) by abuse of notation. Once we have chosen extensions $\mathbf{g}_0 \in \mathbf{H}^{1/2}(\Gamma_{0,D})$ and $\mathbf{h}_0 \in L^2(\Gamma_{0,N})$ of \mathbf{g} and \mathbf{h} , respectively, the defeatured Stokes problem reads:

$$\begin{cases} -\nabla \cdot \$(\mathbf{u}_0) + \nabla p_0 = \mathbf{f} & \text{in } \Omega_0, \\ \nabla \cdot \mathbf{u}_0 = f_c & \text{in } \Omega_0, \\ \mathbf{u}_0 = \mathbf{g}_0 & \text{on } \Gamma_{0,D}, \\ \$\mathbf{u}_0 \mathbf{n} - p_0 \mathbf{n} = \mathbf{h}_0 & \text{on } \Gamma_{0,N}. \end{cases} \quad (25)$$

This problem is well-posed in $V_0(\Omega_0) \times Q_0(\Omega_0)$ with $V_0(\Omega_0) := \mathbf{H}_{\mathbf{g}_0, \Gamma_{0,D}}^1(\Omega_0)$ and $Q_0(\Omega_0) := L^2(\Omega_0)$.

The defeaturing error functions in the velocity and pressure variables are defined by $\mathbf{e}_u := \mathbf{u} - (\mathbf{u}_0)|_{\Omega}$ and $e_p := p - (p_0)|_{\Omega}$, respectively. Moreover, we define the boundary error for each feature by

$$\mathbf{d}_{\gamma^F} := \begin{cases} \mathbf{g}_{|\gamma^F} - (\mathbf{u}_0)_{|\gamma^F}, & F \in \mathcal{F}_D, \\ \mathbf{h}_{|\gamma^F} - (\$(\mathbf{u}_0)\mathbf{n})_{|\gamma^F} - p_0 \mathbf{n}_{|\gamma^F}, & F \in \mathcal{F}_N. \end{cases}$$

As in the Poisson and elasticity cases, an integration by parts argument shows that the defeaturing error can be expressed entirely through boundary terms:

$$\begin{aligned} \|\mathbf{e}_u, e_p\|_{\Omega}^2 &= \sum_{F \in \mathcal{F}_{DD}} \int_{\gamma^F} (\$(\mathbf{e}_u)\mathbf{n} - e_p \mathbf{n}) \cdot \mathbf{d}_{\gamma^F} \, ds \\ &+ \sum_{F \in \mathcal{F}_{D,int}} \int_{\gamma^F} (\$(\mathbf{e}_u)\mathbf{n} - e_p \mathbf{n}) \cdot \mathbf{d}_{\gamma^F} \, ds \\ &+ \sum_{F \in \mathcal{F}_{DN}} \int_{\gamma^F} (\$(\mathbf{e}_u)\mathbf{n} - e_p \mathbf{n}) \cdot \mathbf{d}_{\gamma^F} \, ds + \sum_{F \in \mathcal{F}_N} \int_{\gamma^F} \mathbf{d}_{\gamma^F} \cdot \mathbf{e}_{|\gamma^F} \, ds. \end{aligned} \quad (26)$$

Here, we again make the regularity assumption that $\$(\mathbf{e}_u)\mathbf{n} - e_p \mathbf{n} \in \mathbf{L}^2(\partial\Omega)$. However, the analysis can be conducted under minimal regularity conditions; see Appendix C.

In direct analogy with the Poisson and elasticity cases, the boundary representation motivates the following multi-feature estimator:

$$\begin{aligned} \mathcal{E}_{\mathcal{F}}^{\gamma}(\mathbf{u}_0, p_0) &:= \left(\sum_{F \in \mathcal{F}_{DD}} \mathcal{E}_{DD}^{\gamma^F}(\mathbf{u}_0)^2 + \sum_{F \in \mathcal{F}_{D,int}} \mathcal{E}_{int}^{\gamma^F}(\mathbf{u}_0)^2 \right. \\ &\quad \left. + \sum_{F \in \mathcal{F}_{DN}} \mathcal{E}_{DN}^{\gamma^F}(\mathbf{u}_0)^2 + \sum_{F \in \mathcal{F}_N} \mathcal{E}_N^{\gamma^F}(\mathbf{u}_0, p_0)^2 \right)^{\frac{1}{2}}, \end{aligned} \quad (27)$$

with the feature-wise estimators

$$\mathcal{E}_N^{\gamma^F}(\mathbf{u}_0, p_0) := \left(|\gamma^F|^{\frac{1}{n-1}} \|\mathbf{d}_{\gamma^F} - \overline{\mathbf{d}_{\gamma^F}}^{\gamma^F}\|_{0,\gamma^F}^2 + c_{\gamma^F}^2 |\gamma^F|^{\frac{n}{n-1}} \|\overline{\mathbf{d}_{\gamma^F}}^{\gamma^F}\|_{\ell^2}^2 \right)^{\frac{1}{2}}, \quad (28)$$

$$\mathcal{E}_{DD}^{\gamma^F}(\mathbf{u}_0) := 8\sqrt{\|\mathbf{d}_{\gamma^F}\|_{0,\gamma^F} \|\nabla_t \mathbf{d}_{\gamma^F}\|_{0,\gamma^F}}, \quad (29)$$

$$\mathcal{E}_{DN}^{\gamma^F}(\mathbf{u}_0) := 8\sqrt{\|\mathbf{d}_{\gamma^F} - \overline{\mathbf{d}_{\gamma^F}}^{\gamma^F}\|_{0,\gamma^F} \|\nabla_t \mathbf{d}_{\gamma^F}\|_{0,\gamma^F}} + 8|\gamma^F|^{\frac{n-2}{2(n-1)}} \|\overline{\mathbf{d}_{\gamma^F}}^{\gamma^F}\|_{\ell^2}, \quad (30)$$

$$\mathcal{E}_{int}^{\gamma^F}(\mathbf{u}_0) := 8\sqrt{\|\mathbf{d}_{\gamma^F} - \overline{\mathbf{d}_{\gamma^F}}^{\gamma^F}\|_{0,\gamma^F} \|\nabla_t \mathbf{d}_{\gamma^F}\|_{0,\gamma^F}} + 4\bar{c}_{\gamma^F} \|\overline{\mathbf{d}_{\gamma^F}}^{\gamma^F}\|_{\ell^2}. \quad (31)$$

The reliability of (28) for Neumann features was shown by Antolín and Chanon.² For the proof of reliability of the estimators for Dirichlet features (29) to (31), we refer to Theorem C.2 in Appendix C. The reliability for the estimator expressions (28) to (31) immediately imply the reliability of the multi-feature estimator (27), i.e. we have $\|(\mathbf{e}_u, e_p)\|_{\Omega} \lesssim \mathcal{E}_{\mathcal{F}}^{\gamma}(\mathbf{u}_0, p_0)$.

We consider now a linear QoI $L \in V(\Omega)'$ for the velocity variable with a defeatured counterpart $L_0 \in V_0(\Omega)'$ such that Assumption 2.1 is satisfied. Then, the exact and defeatured dual problems, respectively, read

$$\begin{cases} -\nabla \cdot \mathbf{s}(\mathbf{z}) + \nabla \zeta = L & \text{in } \Omega, \\ \nabla \cdot \mathbf{z} = 0 & \text{in } \Omega, \\ \mathbf{z} = \mathbf{0} & \text{on } \Gamma_D, \\ \mathbf{s}(\mathbf{z})\mathbf{n} - \zeta \mathbf{n} = \mathbf{0} & \text{on } \Gamma_N, \end{cases} \quad (32)$$

and

$$\begin{cases} -\nabla \cdot \mathbf{s}(\mathbf{z}_0) + \nabla \zeta_0 = L_0 & \text{in } \Omega, \\ \nabla \cdot \mathbf{z}_0 = 0 & \text{in } \Omega, \\ \mathbf{z}_0 = \mathbf{0} & \text{on } \Gamma_{0,D}, \\ \mathbf{s}(\mathbf{z}_0)\mathbf{n} - \zeta_0 \mathbf{n} = \mathbf{0} & \text{on } \Gamma_{0,N}. \end{cases} \quad (33)$$

For Stokes' equations, we define the corrector term

$$\begin{aligned} R_L^{\gamma}(\mathbf{u}_0, p_0, \mathbf{z}_0, \zeta_0) := & \sum_{F \in \mathcal{F}_N} \int_{\gamma^F} \mathbf{d}_{\gamma^F} \cdot (\mathbf{z}_0)|_{\gamma^F} \, ds \\ & - \sum_{F \in \mathcal{F}_{DD}} \int_{\gamma^F} (\mathbf{s}(\mathbf{z}_0)\mathbf{n} - \zeta_0 \mathbf{n}) \cdot \mathbf{d}_{\gamma^F} \, ds \\ & - \sum_{F \in \mathcal{F}_{D,int}} \int_{\gamma^F} (\mathbf{s}(\mathbf{z}_0)\mathbf{n} - \zeta_0 \mathbf{n}) \cdot \mathbf{d}_{\gamma^F} \, ds \\ & - \sum_{F \in \mathcal{F}_{DN}} \int_{\gamma^F} (\mathbf{s}(\mathbf{z}_0)\mathbf{n} - \zeta_0 \mathbf{n}) \cdot \mathbf{d}_{\gamma^F} \, ds. \end{aligned}$$

Finally, we can repeat the same argument as for the Poisson and linear elasticity problems in sections 3 and 4 to obtain the following result:

Theorem 5.1. *Let Ω be a Lipschitz domain with negative isotropic Lipschitz features \mathcal{F} . Let $L \in V(\Omega)'$ and $L_0 \in V_0(\Omega)'$ be linear QoIs such that Assumption 2.1 is satisfied. Furthermore, let (\mathbf{u}, p) and (\mathbf{u}_0, p_0) be the solutions to the exact problem (22) and defeatured problem (25), respectively, and (\mathbf{z}_0, ζ_0) the solution to the defeatured dual problem (33). Then, the following estimate holds:*

$$|L(\mathbf{u}) - L_0(\mathbf{u}_0) - R_L^\gamma(\mathbf{u}_0, p_0, \mathbf{z}_0, \zeta_0)| \lesssim \mathcal{E}_{\mathcal{F}}^\gamma(\mathbf{u}_0, p_0) \mathcal{E}_{\mathcal{F}}^\gamma(\mathbf{z}_0, \zeta_0).$$

Remark 5.2. *A similar estimate can be obtained by the same argument for a linear QoI satisfying Assumption 2.1 in the pressure variable. We omit this for brevity.*

6. Numerical experiments

We now validate the theoretical framework through numerical experiments for the Poisson, linear elasticity, and Stokes problems, assessing the reliability and performance of the goal-oriented estimators. The computational geometries and meshes were created with `gmsh`.¹⁵ Crucially, `gmsh` generates meshes that are conformal across lower-dimensional entities, allowing for the simultaneous meshing of the defeatured and exact geometries. In particular, comparing the defeatured to the exact solution is straightforward.

The finite element simulations were implemented with the help of the `FEniCSx` library.³ Local mesh refinement around the features and higher-order elements were used to ensure that the numerical errors could mostly be neglected. For Stokes' equations, Taylor-Hood elements were used to guarantee stability. However, we emphasize that the error estimation framework presented in this paper does not depend on the discretization method or the geometry, as long as numerical integration can be performed along the feature boundaries.

The *effectivity index* $\eta_{\text{eff}} := \mathcal{E}_{\mathcal{F}}^\gamma(\mathbf{u}_0)/\|\mathbf{u}\|_\Omega$ will be used to analyze the performance of the estimators. Indeed, according to the theory, this quantity should be asymptotically independent of the feature size in the limit $|\gamma| \rightarrow 0$. Furthermore, it captures geometric properties that were neglected in the analysis, such as the curvature of the feature boundary.

6.1. Poisson's equation

We start by considering two cases for the Poisson equation in different domains illustrated in Fig. 3: One in the unit square $\Omega_0 = [-\frac{1}{2}, \frac{1}{2}]^2$ with a feature cut out from the boundary (Fig. 3a) and another one in the same unit square with an internal feature cut out at the center (Fig. 3b). In both experiments, we prescribe homogeneous Dirichlet boundary conditions on all defeatured boundaries and the source term is given by

$$f(\mathbf{x}) = \frac{A}{\sqrt{2\pi\sigma^2}} \exp\left(-\frac{1}{2\sigma^2} \|\mathbf{x}\|_{\ell^2}^2\right),$$

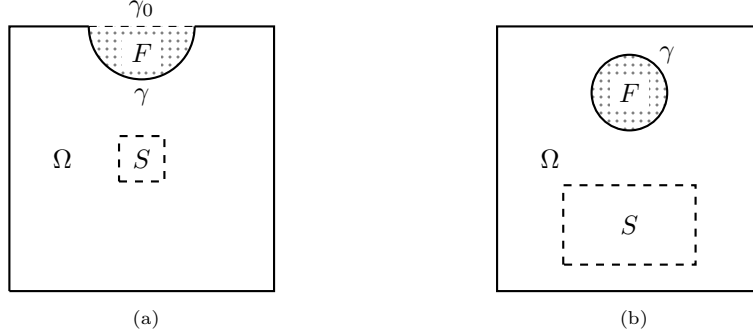


Fig. 3: Illustration of the geometries for the Poisson experiments. The dashed square S represents the integration region for the QoI, while the dotted areas F represent the negative feature cut out from the defeatured domain.

with $A = 10$ and $\sigma^2 = 0.01$. We extend the source term to Ω_0 by the same expression for the defeatured problems. Furthermore, the QoI is given by the expression

$$L(v) = \int_S v \, d\mathbf{x},$$

where the region S varies between experiments.

6.1.1. A feature on the boundary

In this first experiment, we consider a feature on the boundary, for which we must yet prescribe a Dirichlet boundary condition. We impose the condition

$$g(\theta) = \sin(\theta), \quad \theta = \arctan\left(\frac{x_2 - \frac{1}{2}}{x_1}\right), \quad \mathbf{x} = [x_1, x_2]^\top \in \gamma,$$

which is compatible with the homogeneous Dirichlet boundary conditions on the neighboring boundaries. This boundary condition will introduce a strong singularity in the solution u in the exact domain Ω . In this example, the area of influence S is given by

$$S = \{\mathbf{x} \in \mathbb{R}^2 \mid |x_1| \leq \frac{1}{4}, |x_2| \leq \frac{1}{4}\}.$$

Fig. 4 plots the results for the QoI and the different defeaturing errors against the feature size $|\gamma| \in [10^{-3}, \frac{1}{4}]$. More precisely, Figs. 4a and 4c show that the estimate for the QoI error is reliable and that the relative error in the QoI vanishes rapidly in this experiment for $|\gamma| \rightarrow 0$. In contrast, while Fig. 4b shows that the estimates in the primal and dual variables are reliable, the relative defeaturing error in the primal variable remains approximately constant at 100%. The latter is due to the singularity introduced by our specific choice of boundary conditions.

In Fig. 4d, the effectivity indices for the primal and dual variables, as well as the corrected QoI, are plotted. They are indeed asymptotically constant in the

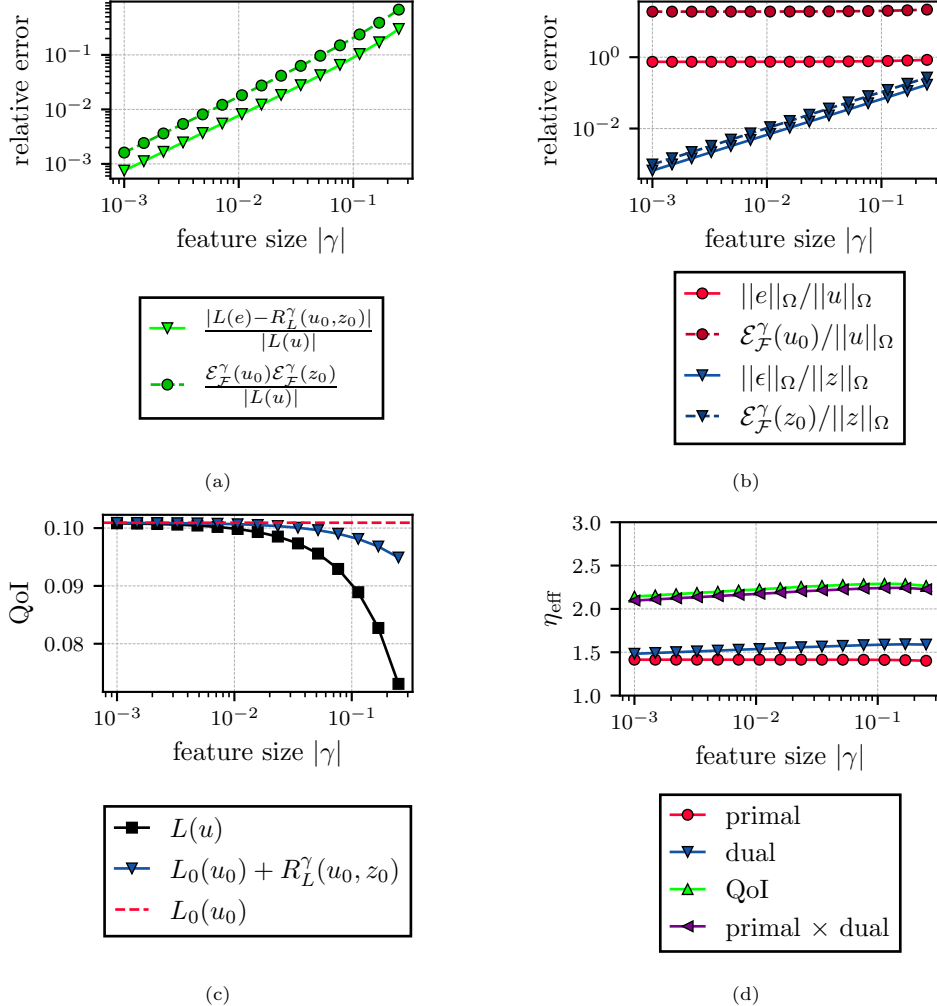


Fig. 4: Results for the Poisson experiment with boundary feature: (a) relative QoI errors and estimates, (b) relative primal and dual defeaturing errors and estimates, (c) QoI values, (d) effectivity indices.

limit $|\gamma| \rightarrow 0$. The slight drop at the lower end can be attributed to the numerical error, as resolving such small features is challenging and requires strong local mesh refinement, especially for the non-smooth dual problem. Furthermore, the effectivity index of the QoI estimate is indeed the product of the effectivity index of the primal and dual variables.

This experiment demonstrates that in general the energy-norm error is a poor proxy for the error in the QoI, underscoring the need for a goal-oriented estimate.

6.1.2. An internal feature

In this experiment, we also impose homogeneous Dirichlet boundary conditions on the feature boundary γ , such that no singularity is introduced at the feature boundary, in contrast to the first example. The area of influence S is given by

$$S = \{\mathbf{x} \in \mathbb{R}^2 \mid |x_1| \leq \frac{1}{4}, -0.4 \leq x_2 \leq -0.15\}.$$

For an inclusion subject to Dirichlet boundary conditions in Poisson problems, it is well-known from singular perturbation theory that the convergence of the defeatured solution u_0 to u is extremely slow if the source term is extended naively into the inclusion,²⁹ i.e. we have $\|u - (u_0)_{|\Omega}\|_{\Omega} \simeq \mathcal{O}(|\log|\gamma||^{-1/2})$ for $\Omega \subset \mathbb{R}^2$. Naturally, the same is true for the dual solutions z and z_0 . Hence, we expect both substantial discrepancies in the energy norm of the primal and dual variables as well as the difference between the exact QoI $L(u)$ and the corrected defeatured QoI $L_0(u_0) + R_L^{\gamma}(u_0, z_0)$ in this case.

However, singular perturbation theory also provides first-order approximations to u and z as follows: Let $\hat{G}(x) = \frac{1}{2\pi} \log(|x - m_F|)$ denote the fundamental solution of the Laplacian centered at the feature's barycenter m_F and consider $G(x) = \hat{G}(x) + g(x)$, where g is the solution to

$$\begin{cases} -\Delta g = 0, & \text{in } \Omega_0, \\ g(x) = -\hat{G}(x) & \text{on } \Gamma_{0,D}, \\ \partial_n g(x) = -\partial_n \hat{G}(x) & \text{on } \Gamma_{0,N}. \end{cases} \quad (34)$$

If the feature F is a disk centered at m_F , the so-called *gauge function* is given by

$$\mu(\gamma) := \frac{2\pi}{\log(\text{diam}(\gamma)/2) - 2\pi\bar{g}^{\gamma}},$$

while for more general shapes, $\mu(\gamma)$ additionally depends on the logarithmic capacity of the feature.^{29,32} Then, the first-order approximations are given by

$$\begin{aligned} u_1(x) &:= u_0(x) + \mu(\gamma) \bar{d}_{\gamma}^{\gamma} G(x), \\ z_1(x) &:= z_0(x) - \mu(\gamma) \bar{z}_0^{\gamma} G(x), \end{aligned}$$

such that $\|u - u_1\|_{\Omega} \simeq \|z - z_1\|_{\Omega} \simeq \mathcal{O}(|\gamma|)$ for $|\gamma| \rightarrow 0$.²⁹

In Fig. 5a, the values of the QoI applied to the exact solution u , the defeatured solution u_0 and the corrected defeatured solution u_1 are plotted for different feature sizes $|\gamma| \in [10^{-3}, \frac{1}{4}]$. We observe that $L_0(u_0)$ remains significantly distant from $L(u)$ across all feature sizes, whereas $L_0(u_1)$ provides a substantially better approximation.

Furthermore, Fig. 5a also shows the corrected QoIs using the corrector term R_L^{γ} applied to different combinations of u_0, u_1, z_0 and z_1 . We observe that when only the zeroth-order approximations u_0 and z_0 are used to reconstruct $L(u)$, the corrector term has no significant impact. This is due to the extremely slow convergence of the zeroth-order approximations in the limit $|\gamma| \rightarrow 0$. Indeed, in Fig. 5b, we see that

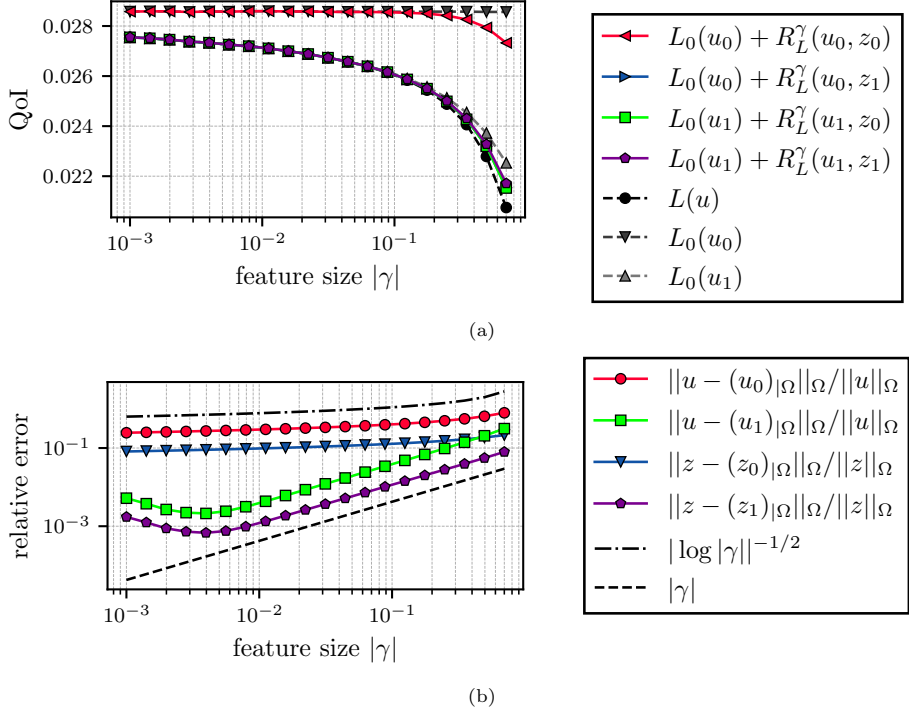


Fig. 5: Results for the Poisson experiment with internal feature: (a) QoI values and (b) relative defeating errors for different approximations of the primal and dual solutions. In (a), the blue line for $L_0(u_0) + R_L^\gamma(u_0, z_1)$ is hidden. In addition, in (b), the convergence rates $\mathcal{O}(|\log |\gamma||^{-1/2})$ and $\mathcal{O}(|\gamma|)$ are plotted for the zeroth- and first-order approximations, respectively.

u_0 and z_0 deviate more than 10% from their respective exact counterparts in the energy norm, even for the smallest feature sizes. Hence, they do not contain enough information for the true QoI to be reconstructed. In contrast, using the first-order approximation in either the primal or dual variable is enough to accurately reconstruct the exact QoI value $L(u)$ using the corrector term R_L^γ . This is reflected by the much faster convergence rate in the limit $|\gamma| \rightarrow 0$ for the first-order approximations in Fig. 5b.

Clearly, the numerical approximation of the first-order approximations becomes increasingly challenging as the feature size approaches zero due to the singularity of the Green's function G , which manifests itself in the increase of their relative errors for small feature sizes in Fig. 5b.

In summary, the goal-oriented estimator is reliable regardless of the energy-norm errors in the primal and dual variables. However, for Dirichlet features, the correction term $R_L^\gamma(u_0, z_0)$ provides additional information to $L_0(u_0)$ only if either u_0 or z_0 is reasonably close to u or z in the energy norm, respectively.

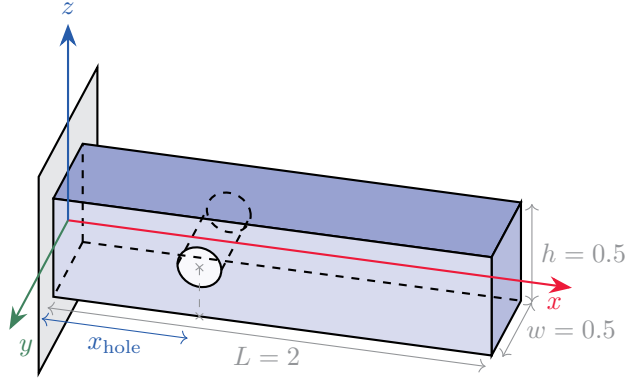


Fig. 6: Illustration of the cantilever beam with a cylindrical hole used in the linear elasticity experiment. The radius of the hole is 0.05 and its x -coordinate x_{hole} is varied between 0.25 and 1.75.

6.2. Linear elasticity

In this section, we consider the linear elasticity problem for the cantilever beam with a cylindrical hole illustrated in Fig. 6. The hole is a negative feature on the boundary in the defeathering context. The Lamé parameters are given by $\mu = 1$ and $\lambda = 1.25$. The beam is clamped at $x = 0$ and subject to gravity. The other boundaries, including the boundary of the hole are kept free. The QoI in this experiment is the average z -displacement at the opposite end of the beam at $x = L$.

Fig. 7 shows the defeathering results for varying x -coordinates of the cylindrical hole $x_{\text{hole}} \in [0.25, 1.75]$. In Fig. 7c, we observe that there is a significant dependence of the exact QoI $L(u)$, which is not captured by the defeatured QoI $L_0(u_0)$. In contrast, the corrected QoI $L_0(u_0) + R_L^\gamma(u_0, z_0)$ closely follows the exact one.

We also note that the estimate is more conservative when the hole is closer to the clamped boundary, which is explained by stronger stress concentrations around the feature in these cases. Indeed, the defeathering error in the energy-norm of the primal variable plotted in Fig. 7b increases when the feature approaches the clamped boundary. Similarly, the error in the corrected QoI increases in Fig. 7a when the feature approaches the clamped boundary as u_0 then provides less and less information through the correction term $R_L^\gamma(u_0, z_0)$.

In contrast, at both extremes of the parameter interval for the feature position, the defeatured QoI deviates significantly from the actual value. At the same time, there is an equilibrium position $x_{\text{hole}} \approx 0.25$, where the feature does not matter at all. For x_{hole} close to 1.75, the estimate even becomes unreliable for the uncorrected QoI $L_0(u_0)$, highlighting the importance of the corrector term.

In addition, we point out that the effectivity index of the goal-oriented estimate is approximately ten for all feature positions, which is coherent with the effectivity indices of the primal and dual variables; see Fig. 7d.

Finally, we observe that in contrast to the Dirichlet features in the Poisson experiments, the corrector term $R_L^\gamma(u_0, z_0)$ adds significant additional information

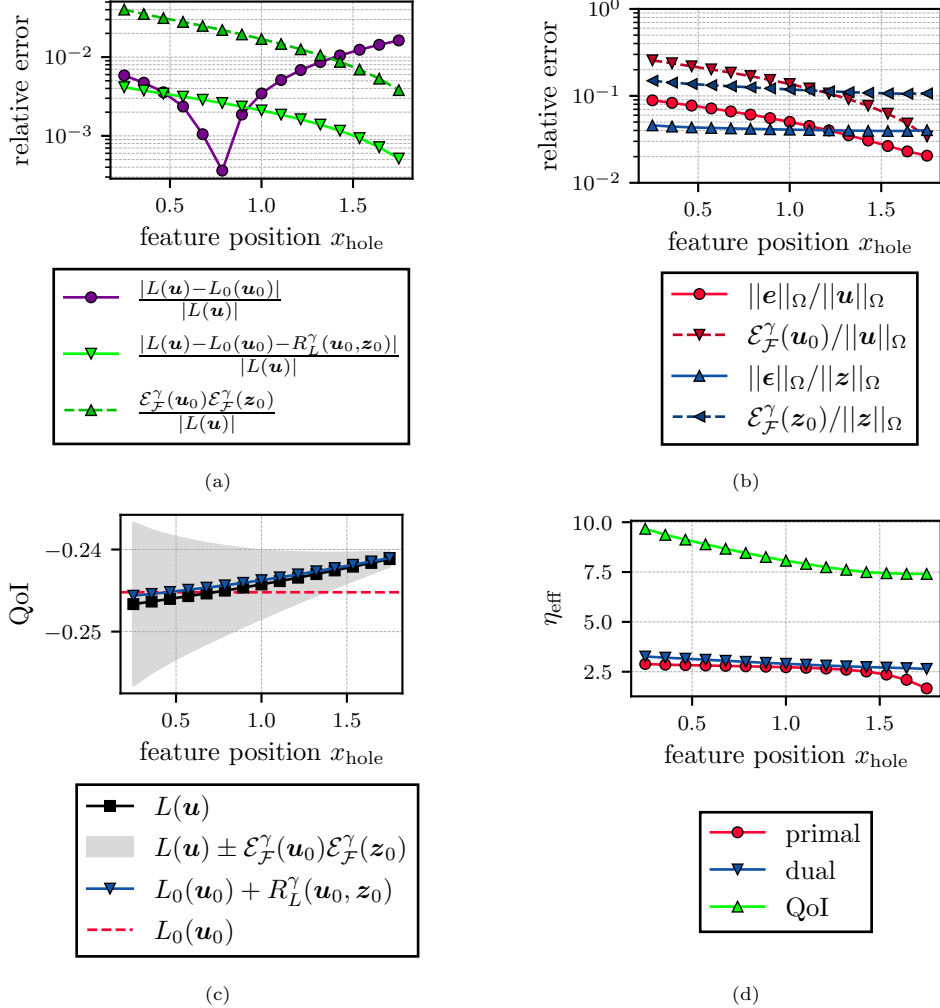


Fig. 7: Results for the linear elasticity experiment for varying feature positions: (a) relative QoI errors and estimates, (b) relative primal and dual defeaturing errors and estimates, (c) QoI values, (d) effectivity indices. In (a), we write $\mathbf{e} := \mathbf{z} - (\mathbf{z}_0)|_\Omega$ for the dual defeaturing error.

to $L_0(\mathbf{u}_0)$ that allows us to estimate the impact of the feature position and shape on L without recomputing the exact solution \mathbf{u} .

6.3. Stokes flow

In this last experiment, we consider Stokes' equations (22) in the domain $\Omega = \Omega_0 \setminus \overline{F}$ illustrated in Fig. 8, where the defeatured domain is the rectangle $\Omega_0 = [-\frac{L}{2}, \frac{L}{2}] \times [-\frac{W}{2}, \frac{W}{2}]$ with $L = 1$ and $W = \frac{1}{2}$. The disk feature F is centered at the origin and its radius will be varied in the interval $[\frac{10^{-3}}{2\pi}, \frac{1}{4\pi}]$.

We prescribe vanishing source terms $\mathbf{f} \equiv \mathbf{0}$ and $f_c \equiv 0$. The bottom and feature

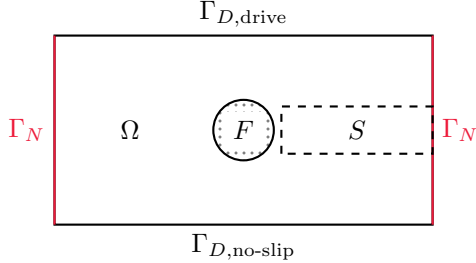


Fig. 8: Illustration of the exact domain Ω with a disk feature F at the center for the Stokes experiment. The bottom boundary $\Gamma_{D,\text{no-slip}}$ and the feature boundary are subject to no-slip conditions, while top boundary $\Gamma_{D,\text{drive}}$ is driven by a constant velocity. The free Neumann boundary Γ_N are marked in red. The dashed rectangle S marks the integration region for the QoI.

boundaries are subject to no-slip boundary conditions, while the lid is driven by a constant velocity $U_x = 1$ in x -direction. The left and right boundaries Γ_N are kept free, i.e. $\mathbf{s}(\mathbf{u})\mathbf{n} - p\mathbf{n} = \mathbf{0}$. This setup leads to a linear flow profile along the y -axis in the defeatured domain, which is perturbed by the circular hole in the exact domain.

The QoI for this experiment is the average x -velocity in the region $S = [\frac{L}{10}, L] \times [-\frac{W}{8}, \frac{W}{8}]$:

$$L(\mathbf{u}) = \int_S u_1 \, dx.$$

Fig. 9c displays the QoI values for various feature sizes alongside the defeatured and corrected approximations. We note that, similar to the Poisson example with the interior feature (cf. Fig. 5a), the corrector term does not provide additional information for the QoI reconstruction.

Nevertheless, Figs. 9a and 9b show that both the goal-oriented estimator and the energy-norm estimator for Dirichlet features in Stokes problems are reliable. Moreover, we note that the error in the QoI does not decrease rapidly in this example. Indeed, as shown in Fig. 9a, the relative error remains above 10% even for the smallest feature size. In addition, we observe in Fig. 9d that the effectivity index is asymptotically independent of the feature size as predicted by the theory.

Finally, we conclude from this example that the defeaturing error in the QoI does not necessarily vanish rapidly as the feature size approaches zero. Hence, geometry simplifications, which are based solely on the size of the feature, are in general inadequate for guaranteeing a prescribed error threshold in the QoI.

7. Conclusion

This work establishes a mathematically certified framework for goal-oriented a posteriori error control in geometric defeaturing. By combining the dual-weighted residual (DWR) method^{4,30} with rigorous energy-norm estimates, we derive certified error bounds for linear quantities of interest (QoIs). Our contributions are threefold: we established new reliable energy-norm estimators for Dirichlet features in linear

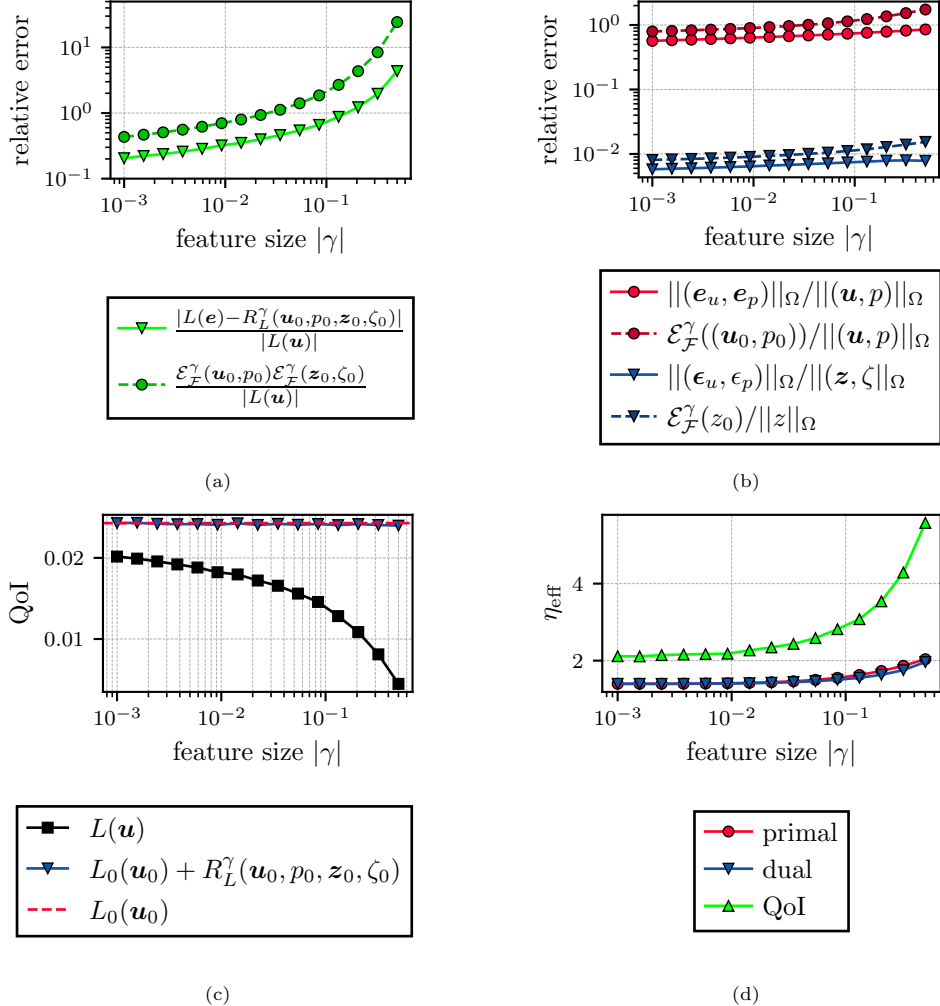


Fig. 9: Results for the Stokes' flow experiment for varying feature positions: (a) relative QoI errors and estimates, (b) relative primal and dual defeaturing errors and estimates, (c) QoI values, (d) effectivity indices. In (b), we write $\epsilon_u := z - (z_0)|_{\Omega}$ and $\epsilon_p := \zeta - (\zeta_0)|_{\Omega}$.

elasticity and Stokes flow; we formulated unified estimators for geometries with mixed feature types; and we derived a certified goal-oriented framework applicable to the Poisson, linear elasticity, and Stokes problems that inherits this generality.

The current framework is limited to negative features. Based on existing estimators for positive Neumann features,¹⁰ the corresponding goal-oriented estimates could be derived similarly. Positive Dirichlet features, however, first require the derivation of energy-norm estimates. Additionally, the current framework only provides an upper bound on the error. While the energy-norm estimates for the Neumann features are known to be efficient,^{7,10} a suitable lower bound remains to be established for Dirichlet features. Hence, future work includes proving the efficiency

of the Dirichlet estimators and developing a suitable framework for positive Dirichlet defeaturering.

The goal-oriented error estimation framework presented in this paper not only establishes a reliable error estimate but also offers a method for reconstructing the exact quantity of interest. This reconstruction is based solely on the defeatured primal and dual solutions, along with the feature boundary information. This approach could open new avenues for shape optimization.

Acknowledgments

This research was supported by the Swiss National Science Foundation via project MINT n. 200021_215099, PDE tools for analysis-aware geometry processing in simulation science.

A. Some results in Sobolev trace spaces

In this section, we collect definitions and results in Sobolev trace spaces that are useful in the context of defeaturering error estimation. For details and proofs, we refer to Chanon,¹⁰ Weder and Buffa³⁸ and Weder.³⁷ Moreover, these definitions and results will be used in the proofs in Appendices B and C.

The following subspace of the trace space $H^{1/2}(\Lambda)$ is essential for our analysis:

$$H_{00}^{1/2}(\Lambda) := \left\{ \mu \in L^2(\Lambda) : \mu^* \in H^{1/2}(\partial\Omega) \right\}, \quad (35)$$

where we write μ^* for the extension of μ by 0 on $\partial\Omega$. The corresponding norm and semi-norm are, respectively, defined by

$$\begin{aligned} \|\mu\|_{H_{00}^{1/2}(\Lambda)}^2 &:= \|\mu\|_{0,\Lambda}^2 + |\mu|_{H_{00}^{1/2}(\Lambda)}^2, \\ |\mu|_{H_{00}^{1/2}(\Lambda)}^2 &:= |\mu|_{1/2,\Lambda}^2 + \int_{\Lambda} \int_{\partial\Omega \setminus \Lambda} \frac{|\mu(y)|^2}{|x-y|^n} ds(x) ds(y). \end{aligned}$$

In particular, we have

$$\|\mu\|_{H_{00}^{1/2}(\Lambda)} = \|\mu^*\|_{1/2,\partial\Omega} \quad \text{and} \quad |\mu|_{H_{00}^{1/2}(\Lambda)} = |\mu^*|_{1/2,\partial\Omega}.$$

These definitions generalize readily to the vector-valued versions of these spaces.

For subsets of the boundary $\Lambda \subset \partial\Omega$ with $|\Lambda| > 0$, we can naturally extend the definition of the Neumann trace operator in (3) to $\nu_n^\Lambda : H(\text{div}; \Omega) \rightarrow H_{00}^{-1/2}(\Lambda)$ by setting

$$\langle \nu_n^\Lambda(v), \mu \rangle := \langle \nu_n(v), \mu^* \rangle, \quad v \in H(\text{div}; \Omega), \mu \in H_{00}^{1/2}(\Lambda). \quad (36)$$

Finally, we point out that one can equip the trace space $H^{1/2}(\partial\Omega)$ with the equivalent natural trace norm given by

$$\|\mu\|_{1/2,\partial\Omega}^{(\text{inf})} := \inf_{u \in H_{\mu,\partial\Omega}^1(\Omega)} \|u\|_{1,\Omega} \quad \forall \mu \in H^{1/2}(\partial\Omega). \quad (37)$$

We refer to Hsiao and Wendland²⁰ for a detailed discussion of equivalent trace space norms.

The following Poincaré and interpolation-type inequalities in trace spaces are crucial for the derivation of the Dirichlet defecting estimators. Although stated for scalar-valued function spaces, these inequalities readily extend to their vector-valued counterparts.

Lemma A.1 (Lemma 2.3.6. in Chanon¹⁰). *Assume that $\Lambda \subset \partial\Omega$ for some Lipschitz domain $\Omega \subset \mathbb{R}^n$. Assume that Λ is isotropic according to Definition 2.1 and connected, and $\partial\Lambda \neq \emptyset$. Then, for all $\mu \in H_{00}^{1/2}(\Lambda)$,*

$$\|\mu\|_{0,\Lambda} \lesssim |\Lambda|^{\frac{1}{2(n-1)}} |\mu^*|_{1/2,\partial\Omega} \leq |\Lambda|^{\frac{1}{2(n-1)}} \|\mu\|_{H_{00}^{1/2}(\Lambda)}.$$

Lemma A.2 (Lemma 2.3.8. in Chanon¹⁰). *Assume that Λ is isotropic according to Definition 2.1. Then, for all $\mu \in H^{1/2}(\Lambda)$,*

$$\|\mu - \bar{\mu}^\Lambda\|_{0,\Lambda} \lesssim |\Lambda|^{\frac{1}{2(n-1)}} |\mu|_{1/2,\Lambda}.$$

Lemma A.3 (Lemma A.4 in Weder and Buffa³⁸). *Assume that Λ is isotropic according to Definition 2.1. Then, for all $\mu \in H^{1/2}(\Lambda)$,*

$$|\mu - \bar{\mu}^\Lambda|_{1/2,\Lambda} \lesssim \sqrt{\|\mu - \bar{\mu}^\Lambda\|_{0,\Lambda} \|\nabla_t \mu\|_{0,\Lambda}},$$

where $\nabla_t \mu$ denotes the gradient in tangential direction. Moreover, if $\mu \in H_{00}^{1/2}(\Lambda)$, we have

$$|\mu|_{H_{00}^{1/2}(\Lambda)} \lesssim \sqrt{\|\mu\|_{0,\Lambda} \|\nabla_t \mu\|_{0,\Lambda}}.$$

Next, we state some results on the norm equivalence between the natural trace space norm defined in (37) and the integral trace norm defined in (1). A detailed discussion of different trace space norms can be found in.²⁰

Proposition A.4 (Proposition 2.5 in Weder and Buffa³⁸). *Let $\Omega \subset \mathbb{R}^n, n \geq 2$ be a domain with Lipschitz boundary $\partial\Omega$ and $\Lambda \subset \partial\Omega$ with $|\Lambda| > 0$. Then, for every $\mu \in H_{00}^{1/2}(\Lambda)$,*

$$\|\mu^*\|_{1/2,\partial\Omega}^{(\text{inf})} \lesssim |\Lambda|^{\frac{-1}{2(n-1)}} \|\mu\|_{0,\Lambda} + |\mu|_{H_{00}^{1/2}(\Lambda)}.$$

Lemma A.5 (Lemma 4.3 in Weder and Buffa³⁸). *Let $\Omega = \Omega_0 \setminus \bar{F} \subset \mathbb{R}^n, n \geq 2$ be a Lipschitz domain with internal Lipschitz feature F and feature boundary $\gamma = \partial F$. We write $\Gamma_0 = \partial\Omega_0$ and we denote by m_F the barycenter of F .*

Then, it holds for $1 \in H_{00}^{1/2}(\gamma)$ that,

$$\|1^*\|_{1/2,\partial\Omega}^{(\text{inf})} \lesssim \bar{c}_\gamma,$$

where

$$\bar{c}_\gamma := \begin{cases} \sqrt{\frac{2\pi}{|\log(s_\gamma)|}}, & n = 2, \\ \sqrt{\frac{2\pi \text{diam}(\gamma)}{1-s_\gamma}}, & n = 3 \end{cases}, \quad \text{and} \quad s_\gamma := \frac{\text{diam}(\gamma)}{2 \text{dist}(m_F, \Gamma_0)}.$$

A generalization of the following result on the operator norm of the partial Neumann trace operator will be used repeatedly in Appendices B and C:

Lemma A.6 (Lemma 2.6 in Weder and Buffa³⁸). *Let $\Omega \subset \mathbb{R}^n, n \geq 2$ be a Lipschitz domain and $\Lambda \subset \partial\Omega$ with $|\Lambda| > 0$ and $\partial\Lambda \neq \emptyset$. Then, it holds for any $v \in H(\text{div}; \Omega)$ and $\mu \in H_{00}^{1/2}(\Lambda)$ that*

$$\langle \nu_n^\Lambda(v), \mu \rangle \lesssim \|v\|_{H(\text{div}; \Omega)} \|\mu\|_{H_{00}^{1/2}(\Lambda)}.$$

Finally, we recall the following extension result on Lipschitz boundaries adapted to the context of deflating error estimation, which is essential for the treatment of Dirichlet-Neumann features. For a detailed proof, we refer to Weder.³⁷

Theorem A.7 (Theorem A.6 in Weder and Buffa³⁸). *Let $\Lambda \subset \mathbb{R}^n$ be a compact $(n-1)$ -dimensional Lipschitz manifold and $\gamma \subset \Lambda$ an $(n-1)$ -dimensional submanifold with boundary. Furthermore, we assume that there exists a subset $\Lambda_0 \subset \Lambda$, such that*

$$\gamma \subset \Lambda_0 \subset \Lambda, \text{ and } \partial\gamma \cap \partial\Lambda = \emptyset.$$

Finally, we assume that the boundary $\partial\gamma$ of γ is an $(n-2)$ -dimensional Lipschitz manifold.

Then, there exists a continuous extension operator $E_\gamma^\Lambda : H^{1/2}(\gamma) \rightarrow H_{00}^{1/2}(\Lambda)$, such that for $\mu \in H^{1/2}(\gamma)$,

$$\|E_\gamma^\Lambda(\mu)\|_{0,\Lambda}^2 \lesssim \|\mu\|_{0,\gamma}^2,$$

and

$$\|E_\gamma^\Lambda(\mu)\|_{1/2,\Lambda}^2 \lesssim |\gamma|^{\frac{-1}{n-1}} \|\mu\|_{0,\gamma}^2 + \|\mu\|_{1/2,\gamma}^2.$$

B. The estimator for Dirichlet features linear elasticity

This appendix is dedicated to proving the reliability of the a posteriori error estimators for Dirichlet features in the linear elasticity problem (18) to (20), as stated in Theorem B.2. The proof follows the same strategy as the one for the Poisson equation presented in Weder and Buffa,³⁸ using key estimates for Sobolev trace spaces from Appendix A.

To that end, it suffices to consider the exact problem (12) and the deflated problem (14) with one single feature of Dirichlet-Dirichlet, Dirichlet-Neumann or internal Dirichlet type. In this simplified case, the deflating error satisfies the following PDE:

$$\begin{cases} -\nabla \cdot \mathbf{s}(\mathbf{e}) = \mathbf{0}, & \text{in } \Omega, \\ \mathbf{s}(\mathbf{e})\mathbf{n} = \mathbf{0}, & \text{on } \Gamma_N, \\ \mathbf{e} = \mathbf{0}, & \text{on } \Gamma_D \setminus \bar{\gamma}, \\ \mathbf{e} = \mathbf{d}_\gamma, & \text{on } \gamma. \end{cases} \quad (38)$$

From an integration by parts and (38), we find that

$$\|\mathbf{e}\|_{\Omega}^2 = \int_{\Omega} \mathbf{s}(\mathbf{e}) : \mathbf{e}(\mathbf{e}) \, dx = \int_{\partial\Omega} \mathbf{s}(\mathbf{e}) \cdot \mathbf{n} \cdot \mathbf{e} \, ds, \quad (39)$$

To arrive at an error estimate, we must carefully study the Neumann trace $\mathbf{s}(\mathbf{e})\mathbf{n}$ on the right-hand side of (39). Accordingly, we define the space

$$\mathbb{H}(\text{div}; \Omega) := \{\mathbf{s} \in \mathbb{L}^2(\Omega) : \nabla \cdot \mathbf{s} \in \mathbf{L}^2(\Omega)\},$$

equipped with the norm

$$\|\mathbf{s}\|_{\mathbb{H}(\text{div}; \Omega)}^2 := \|\mathbf{s}\|_{0,\Omega}^2 + \|\nabla \cdot \mathbf{s}\|_{0,\Omega}^2.$$

Then, the Neumann operator for the linear elasticity problem, $\boldsymbol{\nu}_n : \mathbb{H}(\text{div}; \Omega) \rightarrow \mathbf{H}^{-1/2}(\partial\Omega)$, is defined by integration by parts,

$$\langle \boldsymbol{\nu}_n(\mathbf{s}), \boldsymbol{\mu} \rangle := \int_{\Omega} (\nabla \cdot \mathbf{s}) \cdot \boldsymbol{\phi}_{\boldsymbol{\mu}} \, dx + \int_{\Omega} \mathbf{s} : \mathbf{e}(\boldsymbol{\phi}_{\boldsymbol{\mu}}) \, dx, \quad (40)$$

for some $\boldsymbol{\phi}_{\boldsymbol{\mu}} \in \mathbf{H}_{\boldsymbol{\mu}, \partial\Omega}^1(\Omega)$. This construction is similar to the one for the standard Neumann operator in Girault and Raviart.¹⁶ This operator is clearly continuous since the Cauchy-Schwarz inequality yields

$$\begin{aligned} \langle \boldsymbol{\nu}_n(\mathbf{s}), \boldsymbol{\mu} \rangle &\leq \|\nabla \cdot \mathbf{s}\|_{0,\Omega} \|\boldsymbol{\phi}_{\boldsymbol{\mu}}\|_{0,\Omega} \\ &\quad + \|\mathbf{s}\|_{0,\Omega} \|\boldsymbol{\phi}_{\boldsymbol{\mu}}\|_{1,\Omega} \leq \|\mathbf{s}\|_{\mathbb{H}(\text{div}; \Omega)} \|\boldsymbol{\phi}_{\boldsymbol{\mu}}\|_{1,\Omega}. \end{aligned}$$

Taking the infimum over all possible liftings $\boldsymbol{\phi}_{\boldsymbol{\mu}}$, we obtain

$$\langle \boldsymbol{\nu}_n(\mathbf{s}), \boldsymbol{\mu} \rangle \leq \|\mathbf{s}\|_{\mathbb{H}(\text{div}; \Omega)} \|\boldsymbol{\mu}\|_{1/2, \partial\Omega}^{(\text{inf})},$$

which proves the continuity with respect to the equivalent natural trace space norm (37). Given a subset $\Lambda \subset \partial\Omega$ with $|\Lambda| > 0$, we may define the partial Neumann operator onto Λ as $\boldsymbol{\nu}_n^{\Lambda} : \mathbb{H}(\text{div}; \Omega) \rightarrow \mathbf{H}_{00}^{-1/2}(\Lambda)$ with

$$\langle \boldsymbol{\nu}_n^{\Lambda}(\mathbf{s}), \boldsymbol{\mu} \rangle := \langle \boldsymbol{\nu}_n(\mathbf{s}), \boldsymbol{\mu}^* \rangle, \quad (41)$$

where $\boldsymbol{\mu}^*$ denotes the extension by zero of $\boldsymbol{\mu}$ to $\mathbf{H}^{1/2}(\partial\Omega)$.

Remark B.1. *We point out that if Λ itself has a boundary, then a result similar to Lemma A.6 holds for $\boldsymbol{\nu}_n^{\Lambda}$ asserting that its operator norm does not depend on the size of Λ .*

Starting from the error representation in (39) and using the Neumann operator introduced in the previous subsection, we have

$$\|\mathbf{e}\|_{\Omega}^2 = \langle \boldsymbol{\nu}_n(\mathbf{s}(\mathbf{e})), \mathbf{e} \rangle.$$

For Dirichlet-Dirichlet and internal features, we have $\mathbf{d}_{\gamma} \in \mathbf{H}_{00}^{1/2}(\gamma)$ and in particular

$$\|\mathbf{e}\|_{\Omega}^2 = \langle \boldsymbol{\nu}_n^{\gamma}(\mathbf{s}(\mathbf{e})), \mathbf{d}_{\gamma} \rangle. \quad (42)$$

For Dirichlet-Neumann features, the boundary error \mathbf{d}_γ is not in $\mathbf{H}_{00}^{1/2}(\gamma)$ in general, but merely in $\mathbf{H}^{1/2}(\gamma)$. Therefore, the previous boundary representation of the error is not valid. However, since the Neumann trace of $\mathbf{s}(\mathbf{e})$ vanishes on Γ_N , we can extend \mathbf{d}_γ to $\mathbf{H}_{00}^{1/2}(\Lambda)$, where

$$\gamma \subset \Lambda \subset \text{int}(\bar{\gamma} \cup \bar{\Gamma_N}),$$

is an open neighborhood of γ in the Neumann boundary. Using the continuous extension operator $\mathbf{E}_\gamma^\Lambda : \mathbf{H}^{1/2}(\gamma) \rightarrow \mathbf{H}_{00}^{1/2}(\Lambda)$ from Theorem A.7, we may thus write

$$\|\mathbf{e}\|_\Omega^2 = \langle \boldsymbol{\nu}_n^\Lambda(\mathbf{s}(\mathbf{e})), \mathbf{E}_\gamma^\Lambda(\mathbf{d}_\gamma) \rangle. \quad (43)$$

We circumvented the latter technicality in the main text by assuming that $\boldsymbol{\nu}_n(\mathbf{s}(\mathbf{e})) \in \mathbf{L}^2(\partial\Omega)$ due to additional regularity of the solution. Let us now prove the reliability result for the linear elasticity problem:

Theorem B.2. *Consider the deflating problem for the linear elasticity equation with one single isotropic Dirichlet feature. Then, the following holds:*

1. *If the feature is of Dirichlet-Dirichlet type, then the estimator (18) is reliable. That is, if $\bar{\gamma} \cap \bar{\Gamma_D} \neq \emptyset$ and $\bar{\gamma} \cap \bar{\Gamma_N} = \emptyset$, then*

$$\|\mathbf{e}\|_\Omega \lesssim \mathcal{E}_{\text{DD}}^\gamma(\mathbf{u}_0).$$

2. *If the feature is of Dirichlet-Neumann type, then the estimator (19) is reliable. That is, if $\bar{\gamma} \cap \bar{\Gamma_N} \neq \emptyset$, then*

$$\|\mathbf{e}\|_\Omega \lesssim \mathcal{E}_{\text{DN}}^\gamma(\mathbf{u}_0).$$

3. *If the feature is internal, then the estimator (20) is reliable. That is, if $\bar{\gamma} \cap (\bar{\partial\Omega} \setminus \bar{\gamma}) = \emptyset$, then*

$$\|\mathbf{e}\|_\Omega \lesssim \mathcal{E}_{\text{int}}^\gamma(\mathbf{u}_0).$$

Proof. To prove assertion 1, we use the boundary representation formula (42), Remark B.1 and Lemma A.1 to find

$$\|\mathbf{e}\|_\Omega^2 = \langle \boldsymbol{\nu}_n^\gamma(\mathbf{s}(\mathbf{e})), \mathbf{d}_\gamma \rangle \lesssim 2\|\mathbf{s}(\mathbf{e})\|_{\mathbb{H}(\text{div}, \Omega)} \|\mathbf{d}_\gamma\|_{H_{00}^{1/2}(\gamma)} \lesssim 2\|\mathbf{e}\|_\Omega \|\mathbf{d}_\gamma\|_{H_{00}^{1/2}(\gamma)}.$$

Applying Lemma A.3 to the last factor and dividing by $\|\mathbf{e}\|_\Omega$ on both sides, we find

$$\|\mathbf{e}\|_\Omega \lesssim 2\sqrt{\|\mathbf{d}_\gamma\|_{0,\gamma} \|\nabla_t \mathbf{d}_\gamma\|_{0,\gamma}},$$

which proves the assertion.

To prove assertion 2, we start from the error representation formula (43). Using the same argument as before, we obtain

$$\begin{aligned} \|\mathbf{e}\|_\Omega^2 &= \langle \boldsymbol{\nu}_n^\Lambda(\mathbf{s}(\mathbf{e})), \mathbf{E}_\gamma^\Lambda(\mathbf{d}_\gamma - \bar{\mathbf{d}}_\gamma^\gamma) + \bar{\mathbf{d}}_\gamma^\gamma \mathbf{E}_\gamma^\Lambda(1) \rangle \\ &\lesssim 2\|\mathbf{e}\|_\Omega \left(|\mathbf{E}_\gamma^\Lambda(\mathbf{d}_\gamma - \bar{\mathbf{d}}_\gamma^\gamma)|_{H_{00}^{1/2}(\Lambda)} + \|\bar{\mathbf{d}}_\gamma^\gamma\|_{\ell^2} |\mathbf{E}_\gamma^\Lambda(1)|_{H_{00}^{1/2}(\Lambda)} \right). \end{aligned} \quad (44)$$

Using the continuity properties of E_γ^Λ stated in Ref. 38[Theorem A.6] and Lemmas A.2 and A.3, we find

$$\begin{aligned} |E_\gamma^\Lambda(\mathbf{d}_\gamma - \bar{\mathbf{d}}_\gamma^\gamma)|_{H_{00}^{1/2}(\Lambda)}^2 &\lesssim |\gamma|^{\frac{1}{n-1}} \|\mathbf{d}_\gamma - \bar{\mathbf{d}}_\gamma^\gamma\|_{0,\Lambda}^2 + |\mathbf{d}_\gamma - \bar{\mathbf{d}}_\gamma^\gamma|_{1/2,\gamma}^2 \\ &\lesssim |\mathbf{d}_\gamma - \bar{\mathbf{d}}_\gamma^\gamma|_{1/2,\gamma}^2 \lesssim \|\mathbf{d}_\gamma - \bar{\mathbf{d}}_\gamma^\gamma\|_{0,\gamma} \|\nabla_t \mathbf{d}_\gamma\|_{0,\gamma}. \end{aligned} \quad (45)$$

Similarly, we find

$$|E_\gamma^\Lambda(1)|_{H_{00}^{1/2}(\Lambda)}^2 \lesssim |\gamma|^{\frac{1}{n-1}} \|1\|_{0,\gamma}^2 \lesssim |\gamma|^{\frac{n-2}{n-1}}. \quad (46)$$

Inserting the estimates (45) and (46) into (44) and simplifying on both sides yields assertion 2.

To prove assertion 3, we start again from the error representation formula (42). However, since the boundary of an internal feature itself does not have a boundary, the Poincaré-type inequality from Lemma A.1 does not hold. Hence, the generalization of Lemma A.6 does not apply. Nevertheless, we find

$$\begin{aligned} \|\mathbf{e}\|_\Omega^2 &= \langle \boldsymbol{\nu}_n^\gamma(\mathbf{s}(\mathbf{e})), \mathbf{d}_\gamma \rangle \\ &\lesssim \|\mathbf{s}(\mathbf{e})\|_{\mathbb{H}(\text{div};\Omega)} \left(\|(\mathbf{d}_\gamma - \bar{\mathbf{d}}_\gamma^\gamma)^\star\|_{1/2,\partial\Omega}^{(\text{inf})} + \|\bar{\mathbf{d}}_\gamma^\gamma\|_{\ell^2} \|1^\star\|_{1/2,\partial\Omega}^{(\text{inf})} \right). \end{aligned}$$

Using the fact that $\|\mathbf{s}(\mathbf{e})\|_{\mathbb{H}(\text{div};\Omega)} \lesssim \|\mathbf{e}\|_\Omega$, we obtain

$$\|\mathbf{e}\|_\Omega \lesssim \|(\mathbf{d}_\gamma - \bar{\mathbf{d}}_\gamma^\gamma)^\star\|_{1/2,\partial\Omega}^{(\text{inf})} + \|\bar{\mathbf{d}}_\gamma^\gamma\|_{\ell^2} \|1^\star\|_{1/2,\partial\Omega}^{(\text{inf})}.$$

Applying Proposition A.4 and Lemma A.2 to the first term, we find

$$\|(\mathbf{d}_\gamma - \bar{\mathbf{d}}_\gamma^\gamma)^\star\|_{1/2,\partial\Omega}^{(\text{inf})} \lesssim |\mathbf{d}_\gamma - \bar{\mathbf{d}}_\gamma^\gamma|_{1/2,\gamma} + |\mathbf{d}_\gamma - \bar{\mathbf{d}}_\gamma^\gamma|_{H_{00}^{1/2}(\gamma)}. \quad (47)$$

Note that for an internal feature, we have $\text{dist}(\partial\Omega \setminus \bar{\gamma}, \gamma) > 0$. Therefore, we can estimate the second term as

$$\begin{aligned} |\mathbf{d}_\gamma - \bar{\mathbf{d}}_\gamma^\gamma|_{H_{00}^{1/2}(\gamma)}^2 &= |\mathbf{d}_\gamma - \bar{\mathbf{d}}_\gamma^\gamma|_{1/2,\gamma}^2 + \int_{\partial\Omega \setminus \gamma} \int_{\gamma} \frac{|\mathbf{d}_\gamma(x) - \bar{\mathbf{d}}_\gamma^\gamma|^2}{|x - y|^n} \, ds(x) \, ds(y) \\ &\lesssim |\mathbf{d}_\gamma - \bar{\mathbf{d}}_\gamma^\gamma|_{1/2,\gamma}^2 + \frac{|\partial\Omega \setminus \gamma|}{\text{dist}(\partial\Omega \setminus \gamma, \gamma)^n} \|\mathbf{d}_\gamma - \bar{\mathbf{d}}_\gamma^\gamma\|_{0,\gamma}^2 \\ &\lesssim |\mathbf{d}_\gamma - \bar{\mathbf{d}}_\gamma^\gamma|_{1/2,\gamma}^2. \end{aligned} \quad (48)$$

The second term on the right-hand side of (47) can be estimated by Lemma A.5. Inserting this estimate into (47) together with (48) and applying once more Lemma A.3 as for the two other expressions yields assertion 3. \square

C. The estimator for Dirichlet features in Stokes' equations

This appendix presents the proof of reliability for the a posteriori error estimators for Dirichlet features (29) to (31) in the Stokes problem, as stated in Theorem C.2. The proof strategy closely follows that of the linear elasticity case in Appendix B,

with one additional consideration: the deflating error in the pressure variable. We first show that the pressure error can be controlled by the velocity error via the inf-sup stability condition of the Stokes problem. With the pressure error bounded, the remainder of the proof focuses on the velocity error and proceeds in direct analogy to the elasticity case, treating each of the three feature types in turn.

We consider the exact problem (22) and the deflated problem (25) with one single Dirichlet feature again. Then the deflating error functions $e_u := \mathbf{u} - (\mathbf{u}_0)|_{\Omega}$ and $e_p := p - (p_0)|_{\Omega}$ in the velocity and pressure variables, respectively, satisfy the PDE problem

$$\begin{cases} -\nabla \cdot \mathbf{s}(e_u) + \nabla e_p = \mathbf{0} & \text{in } \Omega, \\ \nabla \cdot e_u = 0 & \text{in } \Omega, \\ \mathbf{s}(e_u) \mathbf{n} - e_p \mathbf{n} = \mathbf{0} & \text{on } \Gamma_N, \\ e_u = \mathbf{0} & \text{on } \Gamma_D \setminus \bar{\gamma}, \\ e_u = \mathbf{d}_{\gamma} & \text{on } \gamma, \end{cases} \quad (49)$$

with a corresponding weak formulation similar to (23) and (24). From integration by parts and using that $b_{\Omega}(e_u, e_p) = 0$, we find

$$a_{\Omega}(e_u, e_u) = a_{\Omega}(e_u, e_u) + b_{\Omega}(e_u, e_p) = \int_{\partial\Omega} (\mathbf{s}(e_u) \mathbf{n} - e_p \mathbf{n}) \cdot e_u \, ds. \quad (50)$$

As for the linear elasticity problem, we must study the Neumann operator on the right-hand side of (50) to derive energy-norm estimates. To that end, we define the subspace

$$\mathcal{H}(\Omega) := \{(\mathbf{s}, q) \in \mathbb{H}(\text{div}; \Omega) \times L^2(\Omega) \mid -\nabla \cdot \mathbf{s} + \nabla q \in \mathbf{L}^2(\Omega)\},$$

equipped with the norm

$$\|(\mathbf{s}, q)\|_{\mathcal{H}(\Omega)} := \|\mathbf{s}\|_{0,\Omega} + \|q\|_{0,\Omega} + \|-\nabla \cdot \mathbf{s} + \nabla q\|_{0,\Omega}.$$

We define the Neumann operator for the Stokes problem, $\boldsymbol{\eta}_n : \mathcal{H}(\Omega) \rightarrow \mathbf{H}^{-1/2}(\partial\Omega)$ by integration by parts:

$$\langle \boldsymbol{\eta}_n(\mathbf{s}, q), \boldsymbol{\mu} \rangle := \int_{\Omega} (-\nabla \cdot \mathbf{s} + \nabla q) \cdot \boldsymbol{\phi}_{\boldsymbol{\mu}} \, dx + \int_{\Omega} \mathbf{s} : \mathbb{E}(\boldsymbol{\phi}_{\boldsymbol{\mu}}) \, dx,$$

for some $\boldsymbol{\phi}_{\boldsymbol{\mu}} \in \mathbf{H}_{\boldsymbol{\mu}, \partial\Omega}^1(\Omega)$. The continuity of the operator immediately follows from the Cauchy-Schwarz inequality:

$$\langle \boldsymbol{\eta}_n(\mathbf{s}, q), \boldsymbol{\mu} \rangle \leq \|-\nabla \cdot \mathbf{s} + \nabla q\|_{0,\Omega} \|\boldsymbol{\phi}_{\boldsymbol{\mu}}\|_{0,\Omega} + \|\mathbf{s}\|_{0,\Omega} \|\boldsymbol{\phi}_{\boldsymbol{\mu}}\|_{1,\Omega} \leq \|(\mathbf{s}, q)\|_{\mathcal{H}(\Omega)} \|\boldsymbol{\phi}_{\boldsymbol{\mu}}\|_{1,\Omega}.$$

Taking the infimum over all $\boldsymbol{\phi}_{\boldsymbol{\mu}} \in \mathbf{H}_{\boldsymbol{\mu}, \partial\Omega}^1(\Omega)$, we obtain

$$\langle \boldsymbol{\eta}_n(\mathbf{s}, q), \boldsymbol{\mu} \rangle \leq \|(\mathbf{s}, q)\|_{\mathcal{H}(\Omega)} \|\boldsymbol{\mu}\|_{1/2, \partial\Omega}^{(\text{inf})},$$

which proves the continuity with respect to the equivalent natural trace space norm (37). In analogy to the linear elasticity problem, given a subset $\Lambda \subset \partial\Omega$ with $|\Lambda| > 0$, we may define the partial Neumann operator onto Λ as $\boldsymbol{\eta}_n^\Lambda : \mathcal{H}(\Omega) \rightarrow \mathbf{H}_{00}^{-1/2}(\Lambda)$ by

$$\langle \boldsymbol{\eta}_n^\Lambda(\mathbf{s}, q), \boldsymbol{\mu} \rangle := \langle \boldsymbol{\eta}_n(\mathbf{s}, q), \boldsymbol{\mu}^* \rangle,$$

where $\boldsymbol{\mu}^*$ denotes the extension by zero of $\boldsymbol{\mu}$ to $\mathbf{H}^{1/2}(\partial\Omega)$.

Remark C.1. *Similar to the Neumann operator for the linear elasticity problem, if Λ itself has a boundary, then a result similar to Lemma A.6 holds for $\boldsymbol{\eta}_n^\Lambda$ asserting that its operator norm does not depend on the size of Λ .*

Using the boundary representation (50) and the Neumann operator above, we have

$$a_\Omega(\mathbf{e}_u, \mathbf{e}_u) = \langle \boldsymbol{\eta}_n(\mathbf{s}(\mathbf{e}_u)), \mathbf{e}_u \rangle.$$

In the Dirichlet-Dirichlet and internal cases, we have $\mathbf{d}_\gamma \in \mathbf{H}_{00}^{1/2}(\gamma)$ and in particular,

$$a_\Omega(\mathbf{e}_u, \mathbf{e}_u) = \langle \boldsymbol{\eta}_n^\gamma(\mathbf{s}(\mathbf{e}_u)), \mathbf{d}_\gamma \rangle. \quad (51)$$

In the Dirichlet-Neumann case, we must again resort to the alternative error representation

$$a_\Omega(\mathbf{e}_u, \mathbf{e}_u) = \langle \boldsymbol{\eta}_n^\Lambda(\mathbf{s}(\mathbf{e}_u)), \mathbf{E}_\gamma^\Lambda(\mathbf{d}_\gamma) \rangle, \quad (52)$$

where $\gamma \subset \Lambda \subset \text{int}(\bar{\gamma} \cup \bar{\Gamma}_N)$ is an open neighborhood of γ in the Neumann boundary.

Regarding the error in the pressure variable, we first observe that $b_\Omega(\mathbf{v}, e_p) = -a_\Omega(\mathbf{e}_u, \mathbf{v})$ for any $\mathbf{v} \in \mathbf{H}_{0, \Gamma_D}^1(\Omega)$ due to equation (23) of the weak form. Moreover, the Stokes problem satisfies the inf-sup condition¹¹ and, therefore, we have

$$\begin{aligned} \|e_p\|_{0, \Omega} &\lesssim \sup_{\mathbf{v} \in \mathbf{H}_{0, \Gamma_D}^1(\Omega)} \frac{b_\Omega(\mathbf{v}, e_p)}{|\mathbf{v}|_{1, \Omega}} \\ &= \sup_{\mathbf{v} \in \mathbf{H}_{0, \Gamma_D}^1(\Omega)} \frac{-a_\Omega(\mathbf{e}_u, \mathbf{v})}{|\mathbf{v}|_{1, \Omega}} \lesssim |\mathbf{e}_u|_{1, \Omega} \lesssim a_\Omega(\mathbf{e}_u, \mathbf{e}_u)^{\frac{1}{2}}, \end{aligned} \quad (53)$$

Hence, is enough to estimate $a_\Omega(\mathbf{e}_u, \mathbf{e}_u)^{\frac{1}{2}}$. Let us now prove the reliability of the Dirichlet estimators for Stokes' equations:

Theorem C.2. *Consider the deflating problem for the linear elasticity equation with one single Dirichlet feature. Then, the following holds:*

1. *If the feature is of Dirichlet-Dirichlet type, then the estimator (29) is reliable. That is, if $\bar{\gamma} \cap \bar{\Gamma}_D \neq \emptyset$ and $\bar{\gamma} \cap \bar{\Gamma}_N = \emptyset$, then*

$$\|(\mathbf{e}_u, e_p)\|_\Omega \lesssim \mathcal{E}_{\text{DD}}^\gamma(\mathbf{u}_0).$$

2. If the feature is if Dirichlet-Neumann type, then the estimator (30) is reliable. That is, if $\bar{\gamma} \cap \bar{\Gamma}_N \neq \emptyset$, then

$$\|(\mathbf{e}_u, e_p)\|_\Omega \lesssim \mathcal{E}_{\text{DN}}^\gamma(\mathbf{u}_0).$$

3. If the feature is internal, then the estimator (31) is reliable. That is, if $\bar{\gamma} \cap (\bar{\partial}\Omega \setminus \gamma) = \emptyset$, then

$$\|(\mathbf{e}_u, e_p)\|_\Omega \lesssim \mathcal{E}_{\text{int}}^\gamma(\mathbf{u}_0).$$

Proof. We begin with the following observations that hold in all three cases: First, we note that in virtue of the PDE (49) satisfied by the defeaturing error, we have

$$\begin{aligned} \|(\mathbf{s}(\mathbf{e}_u), e_p)\|_{\mathcal{H}(\Omega)} &= \|\mathbf{s}(\mathbf{e}_u)\|_{0,\Omega} + \|e_p\|_{0,\Omega} \\ &\lesssim a_\Omega(\mathbf{e}_u, \mathbf{e}_u)^{\frac{1}{2}} + \|e_p\|_{0,\Omega} = \|(\mathbf{e}_u, e_p)\|_\Omega. \end{aligned} \quad (54)$$

Second, the inf-sup estimate (53) implies that

$$\|(\mathbf{e}_u, e_p)\|_\Omega^2 \leq 2a_\Omega(\mathbf{e}_u, \mathbf{e}_u) + 2\|e_p\|_{0,\Omega}^2 \lesssim 4a_\Omega(\mathbf{e}_u, \mathbf{e}_u). \quad (55)$$

For assertion 1, we start from the error representation formula (51). Similar, to the proof of Theorem B.2, we obtain from Remark C.1 and Lemma A.1 that

$$a_\Omega(\mathbf{e}_u, \mathbf{e}_u) = \langle \boldsymbol{\eta}_n^\gamma(\mathbf{s}(\mathbf{e}_u), e_p), \mathbf{d}_\gamma \rangle \lesssim 2\|(\mathbf{s}(\mathbf{e}_u), e_p)\|_{\mathcal{H}(\Omega)} \|\mathbf{d}_\gamma\|_{H_{00}^{1/2}(\gamma)}.$$

Applying (54) to the first and Lemma A.3 to the second term, we find

$$a_\Omega(\mathbf{e}_u, \mathbf{e}_u) \lesssim 2\|(\mathbf{e}_u, e_p)\|_\Omega \sqrt{\|\mathbf{d}_\gamma\|_{0,\gamma} \|\nabla_t \mathbf{d}_\gamma\|_{0,\gamma}}.$$

Assertion 1 then follows from (55).

For assertion 2, we start from the error representation formula (52). Using (54) and (55), we immediately obtain

$$\begin{aligned} \|(\mathbf{e}_u, e_p)\|_\Omega^2 &\lesssim 4a_\Omega(\mathbf{e}_u, \mathbf{e}_u) = 4\langle \boldsymbol{\eta}_n^\Lambda(\mathbf{s}(\mathbf{e}_u)), \mathbf{E}_\gamma^\Lambda(\mathbf{d}_\gamma) \rangle \\ &\lesssim 8\|(\mathbf{e}_u, e_p)\|_\Omega \left(\|\mathbf{E}_\gamma^\Lambda(\mathbf{d}_\gamma - \bar{\mathbf{d}}_\gamma^\gamma)\|_{H_{00}^{1/2}(\Lambda)} + \|\bar{\mathbf{d}}_\gamma^\gamma\|_{\ell^2} \|\mathbf{E}_\gamma^\Lambda(1)\|_{H_{00}^{1/2}(\Lambda)} \right), \end{aligned}$$

where we have used the same argument as for assertion 2 in the proof of Theorem B.2 in the last step. Assertion 2 then follows from the estimates (45) and (46).

For assertion 3, we similarly find from the error representation formula (51), (54), and (55) that

$$\begin{aligned} \|(\mathbf{e}_u, e_p)\|_\Omega^2 &\lesssim 4a_\Omega(\mathbf{e}_u, \mathbf{e}_u) = 4\langle \boldsymbol{\eta}_n^\gamma(\mathbf{s}(\mathbf{e}_u), e_p), \mathbf{d}_\gamma \rangle \\ &\lesssim 8\|(\mathbf{e}_u, e_p)\|_\Omega \left(\|(\mathbf{d}_\gamma - \bar{\mathbf{d}}_\gamma^\gamma)^\star\|_{1/2,\partial\Omega}^{(\text{inf})} + \|\bar{\mathbf{d}}_\gamma^\gamma\|_{\ell^2} \|1^\star\|_{1/2,\partial\Omega}^{(\text{inf})} \right). \end{aligned}$$

Assertion 3 then follows in the same way as assertion 3 of Theorem B.2. \square

References

1. M. S. Agranovich, *Sobolev Spaces, Their Generalizations and Elliptic Problems in Smooth and Lipschitz Domains*, Springer Monographs in Mathematics (Springer International Publishing, Cham, 2015), iSSN: 1439-7382, 2196-9922.
2. P. Antolín and O. Chanon, Analysis-aware defeaturig of complex geometries with Neumann features, *International Journal for Numerical Methods in Engineering* **125** (2024) e7380.
3. I. A. Baratta, J. P. Dean, J. S. Dokken, M. Habera, J. S. Hale, C. N. Richardson, M. E. Rognes, M. W. Scroggs, N. Sime and G. N. Wells, DOLFINx: The next generation FEniCS problem solving environment, December 2023.
4. R. Becker and R. Rannacher, An optimal control approach to *a posteriori* error estimation in finite element methods, *Acta Numerica* **10** (2001) 1–102.
5. D. Boffi, F. Brezzi and M. Fortin, *Mixed Finite Element Methods and Applications*, volume 44 of *Springer Series in Computational Mathematics* (Springer Berlin Heidelberg, Berlin, Heidelberg, 2013).
6. A. Buffa, O. Chanon, D. Grappein, R. Vázquez and M. Vohralík, An Equilibrated Flux A Posteriori Error Estimator for Defeaturing Problems, *SIAM Journal on Numerical Analysis* **62** (2024) 2439–2458.
7. A. Buffa, O. Chanon and R. Vázquez, Analysis-aware defeaturig: Problem setting and *a posteriori* estimation, *Mathematical Models and Methods in Applied Sciences* **32** (2022) 359–402.
8. A. Buffa, O. Chanon and R. Vázquez, Adaptive analysis-aware defeaturig: the case of Neumann boundary conditions, July 2024, arXiv:2212.05183 [math].
9. A. Buffa, D. Grappein and R. Vázquez, Adaptive refinement in defeaturig problems via an equilibrated flux a posteriori error estimator, March 2025, arXiv:2503.19784 [math].
10. O. G. Chanon, Adaptive analysis-aware defeaturig, PhD Thesis, EPFL, Lausanne, 2022.
11. A. Ern and J.-L. Guermond, *Finite Elements II: Galerkin Approximation, Elliptic and Mixed PDEs*, volume 73 of *Texts in Applied Mathematics* (Springer International Publishing, Cham, 2021).
12. R. Ferrandes, P. Marin, J.-C. Leon and F. Giannini, A posteriori evaluation of simplification details for finite element model preparation, *Computers & Structures* **87** (2009) 73–80.
13. L. Fine, L. Remondini and J.-C. Leon, Automated generation of FEA models through idealization operators, *International Journal for Numerical Methods in Engineering* **49** (2000) 83–108.
14. G. Foucault, P. M. Marin and J.-C. Léon, Mechanical Criteria for the Preparation of Finite Element Models, in *International Meshing Roundtable Conference* (2004).
15. C. Geuzaine and J. Remacle, Gmsh: A 3-D finite element mesh generator with built-in pre- and post-processing facilities, *International Journal for Numerical Methods in Engineering* **79** (2009) 1309–1331.
16. V. Girault and P.-A. Raviart, *Finite Element Methods for Navier-Stokes Equations*, volume 5 of *Springer Series in Computational Mathematics* (Springer Berlin Heidelberg, Berlin, Heidelberg, 1986).
17. S. Gopalakrishnan and K. Suresh, A formal theory for estimating defeaturig-induced engineering analysis errors, *Computer-Aided Design* **39** (2007) 60–68.
18. S. Gopalakrishnan and K. Suresh, Feature sensitivity: a generalization of topological

sensitivity, *Finite Elements in Analysis and Design* **44** (2008) 696–704.

19. P. Grisvard, *Elliptic Problems in Nonsmooth Domains* (Society for Industrial and Applied Mathematics, 2011).
20. G. C. Hsiao and W. L. Wendland, *Boundary Integral Equations*, volume 164 of *Applied Mathematical Sciences* (Springer International Publishing, Cham, 2021).
21. T. Hughes, J. Cottrell and Y. Bazilevs, Isogeometric analysis: CAD, finite elements, NURBS, exact geometry, and mesh refinement, *Computer Methods in Applied Mechanics and Engineering* **194** (2005) 4135–4195.
22. K. W. Lee, T. H. Chong and G.-J. Park, Development of a methodology for a simplified finite element model and optimum design, *Computers & Structures* **81** (2003) 1449–1460.
23. K. Y. Lee, C. G. Armstrong, M. A. Price and J. H. Lamont, A small feature suppression/unsuppression system for preparing B-rep models for analysis, in *Proceedings of the 2005 ACM symposium on Solid and physical modeling* (ACM, Cambridge Massachusetts, 2005), pp. 113–124.
24. G. Leoni, *A First Course in Sobolev Spaces*, volume 181 of *Graduate Studies in Mathematics* (American Mathematical Society, Providence, Rhode Island, 2017).
25. M. Li, S. Gao and R. Martin, Estimating the effects of removing negative features on engineering analysis, *Computer-Aided Design* **43** (2011) 1402–1412.
26. M. Li, S. Gao and K. Zhang, A goal-oriented error estimator for the analysis of simplified designs, *Computer Methods in Applied Mechanics and Engineering* **255** (2013) 89–103.
27. J. L. Lions and E. Magenes, *Non-Homogeneous Boundary Value Problems and Applications* (Springer Berlin Heidelberg, Berlin, Heidelberg, 1972).
28. B. Marussig and T. J. R. Hughes, A Review of Trimming in Isogeometric Analysis: Challenges, Data Exchange and Simulation Aspects, *Archives of Computational Methods in Engineering* **25** (2018) 1059–1127.
29. V. Maz'ya, S. Nazarov and B. A. Plamenevskij, *Asymptotic Theory of Elliptic Boundary Value Problems in Singularly Perturbed Domains* (Birkhäuser Basel, Basel, 2000).
30. S. Prudhomme and J. Oden, On goal-oriented error estimation for elliptic problems: application to the control of pointwise errors, *Computer Methods in Applied Mechanics and Engineering* **176** (1999) 313–331.
31. N. Rahimi, P. Kerfriden, F. Langbein and R. Martin, CAD model simplification error estimation for electrostatics problems, *SIAM Journal on Scientific Computing* **40** (2018) 196–227.
32. T. Ransford, Computation of Logarithmic Capacity, *Computational Methods and Function Theory* **10** (2011) 555–578.
33. J. Tang, S. Gao and M. Li, Evaluating defeathering-induced impact on model analysis, *Mathematical and Computer Modelling* **57** (2013) 413–424.
34. A. Thakur, A. Banerjee and S. Gupta, A survey of CAD model simplification techniques for physics-based simulation applications, *Computer-Aided Design* **41** (2009) 65–80.
35. I. Turevsky, S. Gopalakrishnan and K. Suresh, Defeathering: A posteriori error analysis via feature sensitivity, *International journal for numerical methods in engineering* **76** (2008) 1379–1401.
36. I. Turevsky, S. Gopalakrishnan and K. Suresh, An efficient numerical method for computing the topological sensitivity of arbitrary-shaped features in plate bending, *International journal for numerical methods in engineering* **79** (2009) 1683–1702.

37. P. Weder, Extension Operators for Fractional Sobolev Spaces on Lipschitz Submanifolds, July 2025, arXiv:2507.04869 [math].
38. P. Weder and A. Buffa, Analysis-Aware Defeaturing of Dirichlet Features, August 2025, arXiv:2508.13886 [math].
39. D. R. White, S. Saigal and S. J. Owen, Meshing Complexity of Single Part CAD Models, in *International Meshing Roundtable Conference* (2003).
40. K. Zhang, M. Li and J. Li, Estimation of impacts of removing arbitrarily constrained domain details to the analysis of incompressible fluid flows, *Communications in Computational Physics* **20** (2016) 944–968.